FAST MEMORY EFFICIENT EVALUATION OF SPHERICAL POLYNOMIALS AT SCATTERED POINTS

KAMEN IVANOV AND PENCHO PETRUSHEV

Abstract. A method for fast evaluation of band-limited functions (spherical polynomials) at many scattered points on the unit 2-d sphere is presented. The method relies on the superb localization of the father needlet kernels and their compatibility with spherical harmonics. It is fast, local, memory efficient, numerically stable and with guaranteed (prescribed) accuracy. The speed is independent of the band limit and depends logarithmically on the prescribed accuracy. The method can be also applied for approximation on the sphere, verification of spherical polynomials and for fast generation of surfaces in computer-aided geometric design. It naturally extends to higher dimensions.

1. Introduction

In this paper we take on the problem for effective computation of the values of high degree (> 2000) 2-d spherical polynomials at scattered points on the sphere. We seek an algorithm which is accurate, fast, stable and memory efficient. This problem is important for many areas, where high degree spherical harmonics are employed. A targeted application and motivation for this undertaking is the problem for fast efficient computation of the values of the geoid undulation determined from the Earth Gravitational Model EGM2008 of NGA [22].

The problem for fast evaluation of *spherical* polynomials at many scattered points on the unit sphere $\mathbb{S}^2$ in $\mathbb{R}^3$ is traditionally divided into two subproblems:

(i) Evaluate a spherical polynomial of degree N given by its coefficients at *regular grid points* on $\mathbb{S}^2$;

(ii) Evaluate at many, say J, *scattered points* a spherical polynomial of degree N given its values at regular grid points.

Regular grid points on $\mathbb{S}^2$ will be points which are equally spaced or "Gaussian" with respect to each of their *spherical* coordinates (θ, λ). The mesh size in each coordinate is $O(N^{-1})$, thus the grid with a total of $O(N^2)$ points is compatible with the number of polynomial coefficients, that is $(N+1)^2$ (see §2.2). Regular grid points have the obvious drawback that they congregate near the poles, but this is fully compensated by the possibility of applying fast Fourier methods.

This method is particularly effective when the computation has to be executed many times for a single high degree spherical polynomial.

2000 *Mathematics Subject Classification.* 65T99, 42C10, 33C55, 65D32, 41A55.

Key words and phrases. spherical harmonics, evaluation at scattered points, needlets, fast computation.

The first author has been supported by grant DDVU 02/30 of the Fund for Scientific Research of the Bulgarian Ministry of Education and Science. The second author has been supported by NSF Grant DMS-1211528.

A standard method for solving problem (ii) is by using bi-variate spline interpolation, see e.g. [16]. In principle this method experiences accuracy problems because the spherical spline interpolation is not compatible with spherical harmonics. Consequently, the error of approximation is $O((hN)^r)$, where h is the mesh size, N is the degree of the polynomial being approximated and r is the order of the spline interpolant (the constant depends on the uniform norm of the polynomial). The only ways to improve the accuracy of this method are by decreasing the mesh size h in (i) or by restricting its application to smoother spherical polynomials (spherical polynomials with small high degree coefficients). Decreasing the mesh size h creates sever memory and speed problems, while restricting the application to smoother spherical polynomials is usually not an option.

In this article we focus entirely on problem (ii). We put forward a method for its solution based on the spherical "needlets" introduced in [19, 20]. We propose a new approximation scheme based on "father needlets". These are kernels on the sphere which reproduce high order spherical harmonics and are superbly localized and hence are perfectly well suited for approximation in the uniform norm.

The method requires problem (i) to be solved in advance on a regular grid consisting of $O(N^2)$ points. The father needlets being spherical harmonics friendly allow to achieve the desired accuracy ε_0 using a grid with larger mesh size than when using spline interpolation. This distinctive feature of our method leads to modest requirements on the computer memory size, and hence makes it attractive for *compressed* (memory efficient) evaluation of spherical polynomials. Furthermore, the grid depends only on the polynomial degree N and is independent of the polynomial coefficients and the targeted accuracy. Thus, unlike bi-variate splines, better accuracy can be achieved without solving problem (i) for a new refined grid.

The method is *fast* because it is *local* in the sense that only the polynomial values from a small neighborhood of the point of evaluation are used. More precisely, we determine within an arbitrary precision ε_0 the value of a polynomial at a given point using its values at $\nu = O(\ln^2(1/\varepsilon_0))$ neighboring grid points. Thus the number of operations for solving (ii) is $O(\nu J)$. As the form of ν indicates, one can substantially improve the accuracy by a slight enlargement of the point neighborhood. Moreover the number of floating-point operations does not depend on the polynomial degree! Let us also point out that the method is *numerically stable*.

The method has been implemented in MATLAB 2012b with double-precision variables. Variable precision arithmetic is *not needed* for achieving accuracy 10^{-10} in evaluating spherical polynomials of degree up to ten thousand. The method has been intensively tested for degrees between 500 and 2190 (see §5). These tests (and other experiments with polynomials of degree up to 10 000) confirm the features of our method outlined above. Due to the memory efficiency of our algorithm all computations could be performed in real time on a small PC with 1 GB of RAM.

For comparison we next recall briefly some of the existing in the literature methods for evaluation of spherical polynomials. A direct evaluation of a spherical polynomial of degree N given by its coefficients at $O(N^2)$ grid points has computational complexity $O(N^4)$. Using straightforward separation of variables and appropriate associated Legendre functions recurrence formulas the complexity of problem (i) is reduced to $O(N^3)$ and the algorithm is numerically stable.

The first two-dimensional fast Fourier method on the sphere (for expansion, not evaluation) was developed by Driscoll and Healy [3]. The stability of the original algorithms in [3] was problematic and subsequent efforts were made for their stabilization. Mohlenkamp presented in [17] two algorithms for *approximate* solution of problem (i) with costs $O(N^{5/2}\ln N)$ and $O(N^2(\ln N)^2)$. Another approach based on the multi-pole method for approximate solution of (i) with $O(N^2\ln N)$ operations was proposed by Tygert [28, 29], who asserts [28] that the algorithm is numerically stable. It is currently used by several authors, see e.g. [23, 24].

Another approach to the problem for fast evaluation of spherical polynomials given their coefficients relies on their intermediate representation (approximation) via trigonomatric polynomials in spherical coordinates. It was put forward by Kunis and Potts in [15] and is based on the excellent computational properties of the algorithm for nonequispaced fast Fourier transform developed by Dutt and Rokhlin in [4] . In [15] Kunis and Potts utilize a combination of a discrete Legendre functions transform and the nonequispaced fast Fourier transform to solve the problem for fast evaluation of a spherical polynomial at many scattered points. The discrete Legendre functions transform, however, is in principle unstable and various modifications were designed in order to overcome its instability. This instability makes the application of this approach problematic for high degree spherical polynomials.

The proposed method for evaluation of spherical polynomials reflects our fundamental principle that high degree spherical polynomials are better represented by their values at regular grid points than by their coefficients.

The paper is organized as follows. The formulation of the problem and the theoretical basis for its solution by our method is given in §2. In §3 we discuss all parts of the method, describe the relations between the parameters and present the method in an algorithmic form. In §4 we generalize our method to dimensions $d > 2$ and present some of its applications to other problems. Some numerical experiments are described in §5. Section 6 contains a discussion on the method features. The technical proof of Theorem 3.1 is postponded to the Appendix in Section 7.

We will denote by $c, c_1, c_2, \dots$ positive constants which may vary at every appearance and by $\bar{c}, \tilde{c}, c', c''$ and the alike positive constants which preserve their values throughout the paper. The relation $f \sim g$ between functions f and g means $c_1 f \le g \le c_2 f$, while $f \approx g$ is used when $f/g \to 1$ under an appropriate limit of the argument.

2. Theoretical underpinning of our method

In this section we state precisely the problems of interest to us, collect all related background material and develop the theoretical basis of our solution.

2.1. The problem of spherical polynomial evaluation.

We are interested in the folloing

Problem 1. Given a spherical polynomial Y_N with its coefficients $\{a_{m,n}, b_{m,n}\}$, evaluate $Y_N(x)$ at arbitrary (scattered) points $x \in \mathcal{Z}$, on the sphere $\mathbb{S}^2$ with prescribed precision $\varepsilon_0 > 0$, measured in the uniform norm.

We split this problem into two problems:

Problem 2. Given a spherical polynomial Y_N with its coefficients $\{a_{m,n}, b_{m,n}\}$, evaluate $Y_N(\xi)$ at all points ξ from a regular grid $\mathcal{X}$ on $\mathbb{S}^2$.

Problem 3. Given the values $Y_N(\xi)$ of a spherical polynomial Y_N at regular grid points $\xi \in \mathcal{X}$, evaluate $Y_N(x)$ at arbitrary (scattered) points $x \in \mathcal{Z}$, on the sphere $\mathbb{S}^2$ with precision ε_0.

Regular grid points on $\mathbb{S}^2$ will be points $\{(\theta_k, \lambda_\ell)\}$ in spherical coordinates, where $\{\lambda_\ell\}$ are equally distributed and $\{\theta_k\}$ are equally distributed or "Gaussian". Any rotation of such a set of points will also be deemed regular.

We next define explicitly three sets of regular grid points that we shall use in the following. Given $K, L \geq 1$ we define the sets $\mathcal{X}^{(i)} = \{\xi^{(i)}_{k,\ell} = (\theta^{(i)}_k, \lambda^{(i)}_\ell)\}$, $i = 1, 2$, by

$$\theta^{(1)}_k = \frac{\pi}{K}k,\ k = 0, 1, \ldots, K;\ \lambda^{(1)}_\ell = \frac{2\pi}{L}\ell,\ \ell = 0, 1, \ldots, L-1; \tag{2.1}$$

and

$$\theta^{(2)}_k = \frac{\pi}{K}\left(k - \frac{1}{2}\right),\ k = 1, 2, \ldots, K;\ \lambda^{(2)}_\ell = \frac{2\pi}{L}\ell,\ \ell = 0, 1, \ldots, L-1. \tag{2.2}$$

Here in $\mathcal{X}^{(1)}$ we consider only one node for $k = 0$ (the North Pole) and one node for $k = K$ (the South Pole).

The third regular set $\mathcal{X}^{(3)} = \{\xi^{(3)}_{k,\ell}\}$ is defined via the zeros u_k of the Kth degree Legendre polynomials P_K (given in (2.8) below) as follows

$$\theta^{(3)}_k = \arccos u_k,\ k = 1, 2, \ldots, K;\ \lambda^{(3)}_\ell = \frac{2\pi}{L}\ell,\ \ell = 0, 1, \ldots, L-1. \tag{2.3}$$

The relations between K, L and N above are explained in §3.4.

Methods for solving Problem 2 were discussed in the introduction. In the present paper we focus on Problem 3.

2.2. **Spherical harmonics: Background.** Recall first the relation between the cartesian coordinates (x_1, x_2, x_3) and the spherical coordinates (θ, λ), $0 \leq \theta \leq \pi$, $0 \leq \lambda < 2\pi$, of a point x on the unit 2-d sphere $\mathbb{S}^2$:

$$x = (x_1, x_2, x_3) = (\sin\theta\cos\lambda, \sin\theta\sin\lambda, \cos\theta). \tag{2.4}$$

We shall denote by $x \cdot y$ the inner product of $x, y \in \mathbb{S}^2$ and by $\rho(x, y)$ the geodesic distance (angle) between x and y. If $x, y \in \mathbb{S}^2$ are given in spherical coordinates, e.g. $x = (\theta, \lambda)$, $y = (\theta', \lambda')$, then according to the Spherical Law of Cosines

$$x \cdot y = \cos\rho(x, y) = \cos\theta\cos\theta' + \sin\theta\sin\theta'\cos(\lambda - \lambda'). \tag{2.5}$$

Denote by $\mathcal{H}_n$ ($n \geq 0$) the space of all *spherical harmonics of degree* n on $\mathbb{S}^2$. We refer the reader to [25] and [18] for the basics of spherical harmonics. The standard *orthonormal* basis $\{\tilde{\mathcal{C}}_{m,n}\}_{m=0}^n \cup \{\tilde{\mathcal{S}}_{m,n}\}_{m=1}^n$ for $\mathcal{H}_n$ is defined in terms of the associated Legendre functions of the first kind $P_{m,n}$. Namely, for $x = (\theta, \lambda)$

$$\begin{aligned} \tilde{\mathcal{C}}_{m,n}(x) &= q_{m,n}P_{m,n}(\cos\theta)\cos m\lambda,\ m = 0, 1, \ldots, n, \\ \tilde{\mathcal{S}}_{m,n}(x) &= q_{m,n}P_{m,n}(\cos\theta)\sin m\lambda,\ m = 1, 2, \ldots, n, \end{aligned} \tag{2.6}$$

where the coefficients $q_{m,n}$ are given by

$$q_{0,n} = \sqrt{2n+1};\ q_{m,n} = \sqrt{2(2n+1)\frac{(n-m)!}{(n+m)!}},\ m = 1, \ldots, n, \tag{2.7}$$

and

$$P_{m,n}(u) = (1-u^2)^{m/2}\frac{d^m}{du^m}P_n(u).$$

Here P_n is the nth degree Legendre polynomial normalized by $P_n(1) = 1$, i.e.

$$P_n(u) = \frac{1}{2^n n!}\frac{d^n}{du^n}(u^2-1)^n. \tag{2.8}$$

Then for $m = 0, 1, \ldots, n$, $m' = 0, 1, \ldots, n'$ we have

$$\frac{1}{4\pi}\int_{\mathbb{S}^2} \tilde{\mathcal{C}}_{m,n}(x)\tilde{\mathcal{C}}_{m',n'}(x)\,d\sigma(x) = \frac{1}{4\pi}\int_{\mathbb{S}^2} \tilde{\mathcal{S}}_{m,n}(x)\tilde{\mathcal{S}}_{m',n'}(x)\,d\sigma(x) = \delta_{m,m'}\delta_{n,n'},$$

$$\frac{1}{4\pi}\int_{\mathbb{S}^2} \tilde{\mathcal{C}}_{m,n}(x)\tilde{\mathcal{S}}_{m',n'}(x)\,d\sigma(x) = 0, \tag{2.9}$$

where $\delta_{k,\ell}$ is the Kronecker delta and σ is the standard Lebesgue measure on $\mathbb{S}^2$, which in spherical coordinates is given by

$$d\sigma(x) = \sin\theta\, d\theta\, d\lambda. \tag{2.10}$$

An important property of Legendre polynomials is that the kernel of the orthogonal projector $\mathrm{Proj}_{\mathcal{H}_n} : L^2(\mathbb{S}^2) \to \mathcal{H}_n$ is given by $(2n+1)P_n(x\cdot y)$, i.e.

$$(\mathrm{Proj}_{\mathcal{H}_n} f)(x) = \frac{1}{4\pi}\int_{\mathbb{S}^2} (2n+1)P_n(x\cdot y)f(y)d\sigma(y), \quad f \in L^2(\mathbb{S}^2), \tag{2.11}$$

and hence $P_n(x\cdot y)$ is in $\mathcal{H}_n$ as a function of y for every $x \in \mathbb{S}^2$.

In the standard basis (2.6) a spherical polynomial Y_N of degree at most N is given by its coefficients $\{a_{m,n}, b_{m,n}\}$, i.e.

$$Y_N(x) = \sum_{n=0}^{N}\sum_{m=0}^{n}\left(a_{m,n}\tilde{\mathcal{C}}_{m,n}(x) + b_{m,n}\tilde{\mathcal{S}}_{m,n}(x)\right). \tag{2.12}$$

In sums of this form we shall always assume that the term $b_{0,n}\tilde{\mathcal{S}}_{0,n}(x)$ is missing or, equivalently, $\tilde{\mathcal{S}}_{0,n}(x) = 0$. Note that the number of coefficients in (2.12) is $(N+1)^2$.

Denote by Π_N the set of all spherical polynomials of degree at most N. The spherical polynomials are also known as *band-limited functions* on the sphere. As any spherical polynomial (a linear combination of spherical harmonics) is the restriction to $\mathbb{S}^2$ of an algebraic polynomial in three variables [25, Theorem 2.1, Ch. IV], then

$$f \in \Pi_M,\ g \in \Pi_N \implies fg \in \Pi_{M+N}. \tag{2.13}$$

This property is standard for polynomials but, in general, it is not true for harmonic functions.

From (2.11) we see that the kernel of the orthogonal projector $\mathrm{Proj}_{\Pi_N} : L^2(\mathbb{S}^2) \to \Pi_N$ is given by $\sum_{n=0}^{N}(2n+1)P_n(x\cdot y)$, i.e.

$$(\mathrm{Proj}_{\Pi_N} f)(x) = \frac{1}{4\pi}\int_{\mathbb{S}^2}\sum_{n=0}^{N}(2n+1)P_n(x\cdot y)f(y)d\sigma(y), \quad f \in L^2(\mathbb{S}^2), \tag{2.14}$$

and hence $\mathrm{Proj}_{\Pi_N} f = f$ for every $f \in \Pi_N$.

As usual we denote by $L^p(\mathbb{S}^2)$, $1 \le p \le \infty$, the space of functions defined on $\mathbb{S}^2$ with norm

$$\|f\|_{L^p(\mathbb{S}^2)} = \Big(\frac{1}{4\pi}\int_{\mathbb{S}^2} |f(x)|^p\, d\sigma(x)\Big)^{1/p}.$$

For $p=\infty$ we shall consider both $L^\infty(\mathbb{S}^2)$ and $C(\mathbb{S}^2)$ with the standard modification to sup-norm and max-norm, respectively.

We shall denote by

$$E_N(f)_p = \inf_{Y\in\Pi_N} \|f-Y\|_{L^p(\mathbb{S}^2)} \tag{2.15}$$

the best approximation of $f\in L^p(\mathbb{S}^2)$ from spherical polynomials of degree N.

2.3. **Integral spherical "needlet" operators.** The kernel in (2.14) (whose one-dimensional analog is the Dirichlet kernel) has poor localization. We shall utilize reproducing operators with well localized kernels defined by (cf. (2.14))

$$\mathcal{K}_N(u) = \sum_{n=0}^{\infty} \varphi\Big(\frac{n}{N}\Big)(2n+1)P_n(u), \quad u\in[-1,1], \tag{2.16}$$

where P_n is the Legendre polynomial and φ is a cutoff function, namely,

$$\varphi\in C[0,\infty);\ \varphi(t)=1,\ t\in[0,1];\ 0\le\varphi(t)\le 1,\ t\in[1,1+\tau] \text{ and } \varphi(t)=0,\ t\ge 1+\tau, \tag{2.17}$$

for some $\tau>0$. The value of τ will vary depending on the application, as the standard choice is $\tau=1$ (used in [19, 20, 12]).

The "needlet idea" is to vary the cutoff function φ from (2.17) in order to improve the localization of the kernel. As shown in [19, Theorem 3.5] the kernel $\mathcal{K}_N$ from (2.16) has nearly exponential localization for cutoff functions $\varphi\in C^\infty$:

Theorem 2.1. *Let $\varphi\in C^\infty[0,\infty)$ be a cutoff function from (2.17) for some $\tau>0$. Then for any $k>0$ there is a constant $\bar{c}_{k,\tau}$ such that*

$$|\mathcal{K}_N(\cos\theta)| \le \bar{c}_{k,\tau} N^2 (1+N\theta)^{-k}, \quad 0\le\theta\le\pi. \tag{2.18}$$

The localization of $\mathcal{K}_N$ can be improved to sub-exponential if the cutoff function $\varphi\in C^\infty[0,\infty)$ has "small" derivatives, for instance, if φ satisfies

$$\|\varphi\|_\infty \le \tilde{c}'', \quad \frac{1}{k!}\|\varphi^{(k)}\|_\infty \le \tilde{c}''\left(\tilde{c}'[\ln(e+k-1)]^{1+\beta}\right)^k, \quad k=1,2,\dots \tag{2.19}$$

for some constants $\beta,\tilde{c}',\tilde{c}''>0$. The existence of cutoff functions φ satisfying (2.17) and (2.19) is established in [12, Theorem 3.1] and under more general conditions in [13, Theorem 2.3]. The sub-exponential localization of the kernels $\mathcal{K}_N$ can be stated as the following (see [12, Theorem 5.1]):

Theorem 2.2. *Let φ satisfy (2.17) for some $\tau>0$ and (2.19) with constants $\beta,\tilde{c}',\tilde{c}''>0$. Then the kernels $\mathcal{K}_N$ from (2.16) satisfy*

$$|\mathcal{K}_N(\cos\theta)| \le c'' N^2 \exp\left\{-\frac{c'\beta N\theta}{[\ln(e+N\theta)]^{1+\beta}}\right\}, \quad 0\le\theta\le\pi, \tag{2.20}$$

where $c'=\tilde{c}'c^*$ with $c^*>0$ an absolute constant, and the constant $c''>0$ depends only on τ,β, $\tilde{c}'$, and $\tilde{c}''$.

For each φ from (2.17) we consider the linear operator

$$\widetilde{\Phi}_N f(x) := \frac{1}{4\pi}\int_{\mathbb{S}^2} \mathcal{K}_N(x\cdot y) f(y)\, d\sigma(y) \tag{2.21}$$

with kernel defined by (2.16). Note that projection operator from (2.14) is a limiting case of the operator $\widetilde{\Phi}_N$ as $\tau \to 0$. Also, the kernel $\mathcal{K}_N$ can be viewed as a mollified version of the projection (Dirichlet) kernel from (2.14). Clearly,

$$\widetilde{\Phi}_N f = f \quad \forall f \in \Pi_N; \tag{2.22}$$

$$\widetilde{\Phi}_N f \in \Pi_{N_\tau - 1} \quad \forall f \in L^1(\mathbb{S}^2) \text{ with } N_\tau = \lceil N + \tau N \rceil . \tag{2.23}$$

Furthermore, for C^∞ cutoff functions φ the sequence of operators $\left\{\widetilde{\Phi}_N\right\}_{N=0}^{\infty}$ is uniformly bounded, i.e.

$$\|\widetilde{\Phi}_N f\|_{L^p(\mathbb{S}^2)} \le \bar{c}\|f\|_{L^p(\mathbb{S}^2)}, \quad \forall f \in L^p(\mathbb{S}^2), \quad 1 \le p \le \infty, \tag{2.24}$$

with a constant $\bar{c} \ge 1$ depending only on φ. Inequalities (2.24) follow from

$$\frac{1}{4\pi}\int\limits_{\mathbb{S}^2} |\mathcal{K}_N(x \cdot y)|\, d\sigma(y) = \frac{1}{2}\int\limits_0^\pi |\mathcal{K}_N(\cos\theta)| \sin\theta\, d\theta \le \bar{c}, \quad \forall x \in \mathbb{S}^2, \tag{2.25}$$

which is a consequence of Theorem 2.1 with $k = 3$. In fact, a sufficient condition for (2.25) is $\varphi \in W_\infty^3[0, \infty)$.

2.4. **Discrete spherical "needlet" operators.** To make the operator $\widetilde{\Phi}_N$ from (2.21) computationally feasible we discretize $\widetilde{\Phi}_N$ by using a cubature formula on $\mathbb{S}^2$. We shall utilize cubatures of the form

$$\frac{1}{4\pi}\int\limits_{\mathbb{S}^2} f(y)\, d\sigma(y) \sim \sum_{\xi \in \mathcal{X}} w_\xi f(\xi) \text{ with } w_\xi > 0, \tag{2.26}$$

where $\mathcal{X}$ is a finite set of nodes on $\mathbb{S}^2$. For example, $\mathcal{X}$ can be one of the grids $\mathcal{X}^{(i)}$, $i = 1, 2, 3$, from §2.1. We shall assume that the cubature we use is exact for spherical polynomials of certain degree $M - 1 \in \mathbb{N}$

$$\frac{1}{4\pi}\int\limits_{\mathbb{S}^2} f(y)\, d\sigma(y) = \sum_{\xi \in \mathcal{X}} w_\xi f(\xi) \quad \forall f \in \Pi_{M-1}, \tag{2.27}$$

and there is a companion to $\mathcal{X}$ disjoint partition $\{A_\xi\}_{\xi \in \mathcal{X}}$ of $\mathbb{S}^2$ ($\cup_{\xi \in \mathcal{X}} A_\xi = \mathbb{S}^2$) consisting of measurable sets A_ξ with the properties:

$$A_\xi \subset B(\xi, c_1 M^{-1}) \quad \text{and} \quad w_\xi \le c_2 \sigma(A_\xi), \quad \xi \in \mathcal{X}, \tag{2.28}$$

where $c_1, c_2 > 0$ are constants and $B(x, r) = \{y \in \mathbb{S}^2 : \rho(x, y) < r\}$ denotes the open ball centered at x of radius r.

Applying cubature (2.26) to the integral in (2.21) we get a discrete counterpart to the operator $\widetilde{\Phi}_N$, namely,

$$\Phi_N f(x) := \sum_{\xi \in \mathcal{X}} w_\xi \mathcal{K}_N(x \cdot \xi) f(\xi). \tag{2.29}$$

Furthermore, the superb localization of the kernel $\mathcal{K}_N$, given in Theorems 2.1 and 2.2, implies that most of the terms in (2.29) are very small and this leads us to the idea of introducing the truncated operator

$$\Phi_{N,\delta} f(x) := \sum_{\substack{\xi \in \mathcal{X} \\ \rho(x,\xi) \le \delta}} w_\xi \mathcal{K}_N(x \cdot \xi) f(\xi), \tag{2.30}$$

where $\delta > 0$ is a small parameter.

In the next theorem we collect some properties of Φ_N.

Theorem 2.3. *Let φ satisfy* (2.17) *for some $\tau > 0$ and assume $\mathcal{K}_N$ given by* (2.16) *satisfies* (2.18) *with $k \geq 3$. Let the cubature* (2.26) *satisfy* (2.27)–(2.28) *for some $M > N$. Then Φ_N given by* (2.29) *satisfies:*

$$\Phi_N : \ell^\infty(\mathcal{X}) \to C(\mathbb{S}^2) \text{ is a bounded linear operator;} \tag{2.31}$$

$$\|\Phi_N\|_{\ell^\infty(\mathcal{X})\to C(\mathbb{S}^2)} \leq C, \text{ where } C > 0 \text{ is a constant independent of } N; \tag{2.32}$$

$$\Phi_N f \in \Pi_{N_\tau - 1} \quad \forall f \in \ell^\infty(\mathcal{X}) \text{ with } N_\tau = \lceil N + \tau N \rceil . \tag{2.33}$$

Moreover, if

$$M \geq N + N_\tau, \tag{2.34}$$

then

$$\Phi_N f = f \quad \forall f \in \Pi_N; \tag{2.35}$$

$$\|f - \Phi_N f\|_{C(\mathbb{S}^2)} \leq (\|\Phi_N\| + 1) E_N(f)_\infty \quad \forall f \in C(\mathbb{S}^2). \tag{2.36}$$

Proof. Using (2.29) we get (2.31) with norm

$$\|\Phi_N\|_{\ell^\infty(\mathcal{X})\to C(\mathbb{S}^2)} = \sup_{x\in\mathbb{S}^2} \sum_{\xi\in\mathcal{X}} w_\xi \ |\mathcal{K}_N(x\cdot\xi)|. \tag{2.37}$$

In order to bound the above quantity we set $\eta := c_1 N^{-1}$ with c_1 from (2.28) and let $\mathcal{T}$ be a maximal η-net on $\mathbb{S}^2$, i.e. $\rho(y,z) \geq \eta$ for all $y, z \in \mathcal{T}$ and $\mathcal{T}$ cannot be enlarged. Observe that $\mathbb{S}^2 = \cup_{y\in\mathcal{T}} B(y,\eta)$ and $B(y,\eta/2) \cap B(z,\eta/2) = \emptyset$ for $y, z \in \mathcal{T}$, $y \neq z$.

We now split $\mathcal{X}$ into disjoint subsets $\mathcal{X}_y$, $y \in \mathcal{T}$, so that $\xi \in B(y,\eta)$ for all $\xi \in \mathcal{X}_y$. From the properties of $\{A_\xi\}$, see (2.28), we get for any $y \in \mathcal{T}$

$$\sum_{\xi\in\mathcal{X}_y} w_\xi \leq c_2 \sum_{\xi\in\mathcal{X}_y} \sigma(A_\xi) \leq c_2 \sigma(B(y,2\eta)) \leq cN^{-2}. \tag{2.38}$$

On the other hand, for any $x \in \mathbb{S}^2$, $y \in \mathcal{T}$ and $\xi \in \mathcal{X}_y$ (hence $\xi \in B(y,\eta)$) we have

$$1 + N\rho(x,y) \leq 1 + N\rho(x,\xi) + N\rho(\xi,y) \leq 1 + N\rho(x,\xi) + c_1 \leq c(1 + N\rho(x,\xi)).$$

From this, (2.38), and (2.18) with $k = 3$ we infer

$$\sum_{\xi\in\mathcal{X}_y} w_\xi |K(x\cdot\xi)| \leq c(1 + N\rho(x,y))^{-3}, \quad x \in \mathbb{S}^2, y \in \mathcal{T}.$$

Therefore,

$$\sum_{\xi\in\mathcal{X}} w_\xi |K(x\cdot\xi)| = \sum_{y\in\mathcal{T}} \sum_{\xi\in\mathcal{X}_y} w_\xi |K(x\cdot\xi)| \leq c \sum_{y\in\mathcal{T}} (1 + N\rho(x,y))^{-3}. \tag{2.39}$$

To estimate the last sum above for fixed $x \in \mathbb{S}^2$ we split the set $\mathcal{T}$ by setting $\mathcal{T}_0 := \{y \in \mathcal{T} : \rho(x,y) < 2^{-1}\eta\}$ and $\mathcal{T}_j := \{y \in \mathcal{T} : 2^{j-2}\eta \leq \rho(x,y) < 2^{j-1}\eta\}$, $j \geq 1$. Clearly,

$$c\eta^2 \# \mathcal{T}_j \leq \sum_{y\in\mathcal{T}_j} \sigma(B(y,\eta/2)) \leq \sigma(B(x,2^j\eta)) \leq c' 2^{2j} \eta^2$$

implying $\#\mathcal{T}_j \le c2^{2j}$, $j \ge 1$. Evidently, $\#\mathcal{T}_0 \le 1$. Using these estimates we get

$$\sum_{y\in\mathcal{T}}(1+N\rho(x,y))^{-3} \le \sum_{j\ge 0}\sum_{y\in\mathcal{T}_j}(1+N\rho(x,y))^{-3}$$
$$\le 1 + c\sum_{j\ge 1}2^{-3j}\#\mathcal{T}_j \le 1 + c\sum_{j\ge 1}2^{-j} \le c' < \infty.$$

This coupled with (2.39) yields $\sum_{\xi\in\mathcal{X}} w_\xi |K(x\cdot\xi)| \le C < \infty$. We use this in (2.37) to obtain (2.32).

Property (2.33) follows from (2.29), (2.16) and (2.11).

By (2.13), (2.16) and (2.11) we infer that if $f \in \Pi_N$, then $\mathcal{K}_N(x\cdot\xi)f(\xi)$ is a spherical polynomial of ξ of degree $N + N_\tau - 1$ for every $x \in \mathbb{S}^2$. Now, property (2.35) follows from (2.29), (2.34), (2.27), (2.21) and (2.22). For the proof of (2.36) let Y realize the inf in (2.15) with $p = \infty$. Then

$$\|f - \Phi_N f\|_{C(\mathbb{S}^2)} \le \|f - Y\|_{C(\mathbb{S}^2)} + \|Y - \Phi_N Y\|_{C(\mathbb{S}^2)} + \|\Phi_N(f-Y)\|_{C(\mathbb{S}^2)},$$

which gives (2.36) on account of (2.31) and (2.35). □

Note that Theorem 2.3 holds, in particular, for any C^∞ cutoff function φ. From (2.33), (2.15), (2.36) and (2.32) it follows that

$$E_{N_\tau-1}(f)_\infty \le \|f - \Phi_N f\|_{C(\mathbb{S}^2)} \le cE_N(f)_\infty,$$

which shows the superb approximation properties of operators Φ_N.

Some properties of the operators $\Phi_{N,\delta}$ read as follows:

Theorem 2.4. *Let $\mathcal{K}_N$ satisfy*

$$|\mathcal{K}_N(\cos\theta)| \le \varepsilon \quad \textit{for} \quad \delta \le \theta \le \pi. \tag{2.40}$$

Then under the assumptions of Theorem 2.3 we have

$$\Phi_{N,\delta} : \ell^\infty(\mathcal{X}) \to L^\infty(\mathbb{S}^2) \textit{ is a bounded linear operator}; \tag{2.41}$$

$$\|\Phi_N f - \Phi_{N,\delta} f\|_{L^\infty(\mathbb{S}^2)} \le \varepsilon\|f\|_{\ell^\infty(\mathcal{X})} \quad \forall f \in \ell^\infty(\mathcal{X}); \tag{2.42}$$

$$\|f - \Phi_{N,\delta} f\|_{L^\infty(\mathbb{S}^2)} \le (C+1)E_N(f)_\infty + \varepsilon\|f\|_{\ell^\infty(\mathcal{X})} \quad \forall f \in C(\mathbb{S}^2), \tag{2.43}$$

where C is the constant from (2.32).

Proof. From (2.40) we get

$$\sum_{\substack{\xi\in\mathcal{X}\\ \rho(x,\xi)>\delta}} w_\xi\ |\mathcal{K}_N(x\cdot\xi)| \le \sum_{\substack{\xi\in\mathcal{X}\\ \rho(x,\xi)>\delta}} w_\xi\ \varepsilon \le \varepsilon. \tag{2.44}$$

This along with (2.29)–(2.30) leads to

$$|\Phi_N f(x) - \Phi_{N,\delta} f(x)| \le \sum_{\substack{\xi\in\mathcal{X}\\ \rho(x,\xi)>\delta}} w_\xi\ |\mathcal{K}_N(x\cdot\xi)|\ \|f\|_{\ell^\infty(\mathcal{X})} \le \varepsilon\|f\|_{\ell^\infty(\mathcal{X})}.$$

Now Theorem 2.4 follows immediately from Theorem 2.3 and the above estimate. □

3. Toward an effective computational method

Theorem 2.4 suggests the main steps in solving effectively Problem 3 from §2.1. According to (2.42) with $f = Y_N$ the error of computing (approximating) $Y_N(x)$ by means of $\Phi_{N,\delta}Y_N(x)$, $x \in \mathbb{S}^2$, does not exceed ε_0 if δ is determined in (2.40) with

$$\varepsilon = \varepsilon_0/\|Y_N\|_{\ell^\infty(\mathcal{X})}. \tag{3.1}$$

The quantity $\|Y_N\|_{\ell^\infty(\mathcal{X})}$ can be easily computed as the values $Y_N(\xi)$, $\xi \in \mathcal{X}$, are known. In (3.1) we may consider ε_0 as the absolute error of our method (if the computations are performed in the exact arithmetic), while ε is the relative error (with respect to the polynomial norm, not a particular polynomial value!).

Apparently, the number of operations needed to compute $\Phi_{N,\delta}f(x)$ is a constant multiple of the number of terms in (2.30), which in turn depends on how smaller δ is. Thus varying φ in (2.17) we seek for a given ε the smallest possible δ such that (2.40) holds. Upper and lower bounds for the order of the best possible δ are given in §3.1 and an improved criterion for determining δ is given in §3.2. Note that the choice of δ is independent of the cubature formula (because $\|Y_N\|_{\ell^\infty(\mathcal{X})} \le \|Y_N\|_{C(\mathbb{S}^2)}$). Moreover the dependence of δ on the polynomial Y_N is only via the degree N and the polynomial norm $\|Y_N\|_{C(\mathbb{S}^2)}$.

The problem for fast and accurate computation of the values $\mathcal{K}_N(x \cdot \xi)$ is non-trivial due to fact that the function $\mathcal{K}_N(\cos\rho)$ in (2.30) changes very rapidly for ρ close to 0. Thus the round-off error in the computation of $x \cdot \xi$ by (2.5) may cause undesirable big error in the value of $\mathcal{K}_N(x \cdot \xi)$. In §3.3 we present an effective solution to this problem combined with a very fast method for evaluation of $\mathcal{K}_N(\cos\rho)$.

Having obtained δ we need to determine effectively the nodes $\xi \in \mathcal{X}$ that satisfy $\rho(x,\xi) \le \delta$. This step gives advantage to nodal sets with some kind of structure, e.g. as in (2.1), (2.2) or (2.3). The values of the cubature weights associated with these nodes and the proof that the cubatures satisfy (2.27)–(2.28) are given in §3.4.

As was pointed out in §2.1 the nodes in (2.1), (2.2) and (2.3) get denser around the poles. This means that for x close to one of the poles the sum in (2.30) will have $O(N^2\delta)$ terms as opposed to the normal $O(N^2\delta^2)$ terms for x away from the poles. A simple method for avoiding this undesirable drawback is given in §3.5.

The connection between the degree of exactness of the cubature and the polynomial degree N is only one-sided – via the inequalities $M > N$ or $M \ge N + N_\tau$ in the hypothesis of Theorem 2.3. This means that we can increase the degree of exactness M and thus the number of nodes. If we keep δ fixed, then this will lead to a larger number of nodes in the δ-neighborhood of x and increase the computational cost. Such relation would be inconsistent with the general perception that the knowledge of the polynomial values at larger number of nodes should make the point-wise evaluation easier and faster. In our method in accordance with this idea we can increase the parameter τ in (2.17), which will lead to the decrease of δ and, as a consequence, to smaller number of nodes in the δ-neighborhood of a point. The details are given in §3.6.

All elements of our algorithm for solving Problem 3 are given in §3.7.

3.1. Bounds on δ.

Given $\tau > 0$, a cutoff function φ satisfying (2.17), $0 < \varepsilon \le 1$, and $N \ge 1$ we denote by $\delta_\infty(\varphi;\varepsilon,\tau,N)$ the minimal δ for which (2.40) holds.

Functions φ with small δ are deemed to be good cutoff functions. Set

$$\delta_\infty(\varepsilon,\tau,N)=\inf_{\varphi}\delta_\infty(\varphi;\varepsilon,\tau,N),$$

where the infimum is taken on all φ satisfying (2.17). We are interested in establishing lower and upper bounds on $\delta_\infty(\varepsilon,\tau,N)$.

The upper bound relies on the following

Theorem 3.1. *Let $N,k\in\mathbb{N}$, $N>k$ and $\tau>0$. Let the cutoff function φ be defined by* (7.4). *Then there exist absolute constants $c_0,c_1>0$ such that*

$$|\mathcal{K}_N(\cos\theta)|\le c_0\left((1+\tau)N\right)^2\min\left\{1,\left(\frac{c_1k}{\tau N\theta}\right)^k\right\},\quad \theta\in[0,\pi]. \tag{3.2}$$

This theorem follows by Theorem 7.1 with $\alpha=\beta=0$ from the appendix.

Lower and upper bounds on $\delta_\infty(\varepsilon,\tau,N)$ are given in

Theorem 3.2. *Let $N\in\mathbb{N}$, $0<\varepsilon\le 1$ and $\tau\ge 1$. Then there exist absolute constants $c_1^-,c_1^+,c_2^+>0$ such that for $N>2\max\{\ln(c_0(1+\tau)^2/\varepsilon),4\}$ with c_0 from Theorem 3.1 we have*

$$\frac{c_1^-\ln(N^2/\varepsilon)}{\tau N}\le\delta_\infty(\varepsilon,\tau,N)\le\frac{c_1^+\ln(N^2/\varepsilon)+c_2^+\ln(1+\tau)}{\tau N}. \tag{3.3}$$

Proof. For the lower bound we shall employ the Chebyshev polynomials. By (2.16)–(2.17) it follows that $\mathcal{K}_N$ (defined in (2.16)) is an algebraic polynomial of degree $m=N_\tau-1$ satisfying

$$\mathcal{K}_N(1)=\sum_{n=0}^{m}\varphi\left(\frac{n}{N}\right)(2n+1)=\kappa_{\varphi,N}N^2 \tag{3.4}$$

with $1\le\kappa_{\varphi,N}\le(1+\tau)^2$. As is well known among all algebraic polynomials of degree m with uniform norm 1 on $[-1,1]$ the Chebyshev polynomial of the first kind T_m has the fastest growth for every $v\in(1,\infty)$. By a linear change of the variable we get the following Bernstein inequality: For any $a\in\mathbb{R}$, $b>0$ and any algebraic polynomial P of degree m we have

$$\|P\|_{C[a-vb,a+vb]}\le T_m(v)\|P\|_{C[a-b,a+b]}\quad\forall v\in(1,\infty). \tag{3.5}$$

Therefore, a lower bound δ_0 for δ from (2.40) will be given by the m-th degree polynomial $\tilde{T}_m(u)=\varepsilon T_m((2u+d)/(2-d))$ with $d=1-\cos\delta_0$ and $\tilde{T}_m(1)=\mathcal{K}_N(1)$ because

$$|\tilde{T}_m(\cos\theta)|\le\varepsilon\quad\text{for}\quad\delta_0\le\theta\le\pi\quad\text{and}\quad|\tilde{T}_m(\cos\theta)|>\varepsilon\quad\text{for}\quad 0\le\theta<\delta.$$

From this condition, (3.4) and the standard representation of $T_m(u)$ for $u\ge1$ (see e.g. [2, p. 76]) we obtain the following equation for δ_0

$$\left(v+\sqrt{v^2-1}\right)^m+\left(v-\sqrt{v^2-1}\right)^m=\frac{2\kappa_{\varphi,N}N^2}{\varepsilon},\quad v=\frac{3-\cos\delta_0}{1+\cos\delta_0}. \tag{3.6}$$

The exact explicit solution of (3.6) is

$$\delta_0=\arccos(8S(S+1)^{-2}-1),\quad S=\left(R+\sqrt{R^2-1}\right)^{1/m},\quad R=\frac{\kappa_{\varphi,N}N^2}{\varepsilon}.$$

From the above we get the following asymptotic of δ_0 for large N and small ε

$$\delta_0\approx\frac{\ln(2\kappa_{\varphi,N}N^2/\varepsilon)}{m}>\frac{\ln(2N^2/\varepsilon)}{2\tau N}. \tag{3.7}$$

Now, the inequality $\delta(\varphi;\varepsilon,\tau,N)\ge\delta_0$ coupled with (3.7) gives the lower bound in (3.3).

For the upper bound in (3.3) we apply Theorem 3.1 with $\delta=c_1ek/(\tau N)$ and $k=\lceil\ln(c_0(1+\tau)^2N^2/\varepsilon)\rceil$ (hence $N>k$) to obtain

$$|\mathcal{K}_N(\cos\theta)|\le\varepsilon,\quad \delta\le\theta\le\pi. \tag{3.8}$$

This completes the proof. □

Remark 3.3. In fact, the upper bound in (3.3) holds for $0<\tau<\infty$. The condition $\tau\ge1$ is used only for the inequality in (3.7). For $0<\tau<1$ the denominator of the lower bound in (3.3) is $(1+\tau)N$ and does not match the upper bound. Note that the localization of $\mathcal{K}_N$ gets worse when $\tau\to0$ and necessarily $\delta_\infty(\varepsilon,\tau,N)\to\pi$ in this case.

Remark 3.4. There is no term $c_2^-\ln(1+\tau)$ in the numerator of the lower bound in (3.3) because 1 was used in (3.7) as a lower bound for $\kappa_{\varphi,N}$. The term $c_2^-\ln(1+\tau)$ would appear in the lower bound in (3.3) if φ obeys some mild additional restrictions such as $\varphi(u)\ge c>0$ for $1\le u\le1+\tau/2$.

Remark 3.5. Theorems 2.1 and 3.1 look very similar – both of them state that the "needlet kernel" has a majorant with a power-type decrease. The main difference is that the dependence of constant $\bar c_{k,\tau}$ in Theorem 2.1 on k is not specified while the same constant in Theorem 3.1 behaves as $(ck)^k$ for fixed τ. This behavior of $\bar c_{k,\tau}$ in Theorem 3.1 is achieved by W^k_∞ functions φ which vary with k and implies the very strong upper estimate in (3.3) when $k=\lceil\ln(c_0(1+\tau)^2N^2/\varepsilon)\rceil$. The upper estimate in (3.3) is not true for any single "universal" (i.e. independent on N and ε) cutoff function φ from C^∞, even for those φ satisfying (2.19).

In fact, the kernels $\mathcal{K}_N$ generated by different cutoff functions in Theorems 2.1, 2.2 and 3.1 belong to the class of fast decreasing polynomials studied in Ivanov, Totik [14].

3.2. **An improved criterion for δ.** The majorants of $|\mathcal{K}_N(\cos\theta)|$ given in (2.18), (2.20) and (3.2), after reaching the value ε for $\theta=\delta_\infty$, preserve their fast decay for $\theta>\delta_\infty$. This means that it is possible to select a smaller value of δ in the operator $\Phi_{N,\delta}$ from (2.30) and still have the same error bound as in (2.42). This can be achieved, for example, by replacing the uniform condition in (2.40) by an integral one. Thus we arrive at the equation

$$\frac12\int_{-1}^{\cos\delta}|\mathcal{K}_N(u)|\,du=\varepsilon\quad\left(=\frac{\varepsilon}{2}\int_{-1}^{1}\mathcal{K}_N(u)\,du\right), \tag{3.9}$$

which determines $\delta=\delta_1(\varphi;\varepsilon,\tau,N)$ as a function of ε, τ, N and φ (satisfying (2.17)). The fact that the second integral in (3.9) is equal to 2 follows from (2.16) and the orthogonality of Legendre polynomials on $[-1,1]$.

Equation (3.9) is justified by the following approximate identity (cf. (2.44)) for cubatures *with positive weights*:

$$\sum_{\substack{\xi\in\mathcal{X}\\ \rho(x,\xi)>\delta}} w_\xi\ |\mathcal{K}_N(x\cdot\xi)| \cong \frac{1}{4\pi}\int\limits_{\rho(x,\xi)>\delta} |\mathcal{K}_N(x\cdot\xi)|\,d\sigma(\xi) \tag{3.10}$$

$$= \frac{1}{2}\int\limits_{\delta}^{\pi} |\mathcal{K}_N(\cos\theta)|\sin\theta\,d\theta = \frac{1}{2}\int\limits_{-1}^{\cos\delta} |\mathcal{K}_N(u)|\,du = \varepsilon.$$

From (3.10), (2.29) and (2.30) we get immediately the following counterpart of (2.42)

$$\|\Phi_N f - \Phi_{N,\delta} f\|_{L^\infty(\mathbb{S}^2)} \le \varepsilon \|f\|_{\ell^\infty(\mathcal{X})} \quad \forall f\in\ell^\infty(\mathcal{X}) \tag{3.11}$$

for every $\delta\in[\delta_1(\varphi;\varepsilon,\tau,N),\pi]$.

In looking for small δ for the truncated operator $\Phi_{N,\delta}$ from (2.30) we arrived at

Problem 4. For given $\tau>0$, $\varepsilon\in(0,1]$ and $N\ge 1$ set

$$\delta_1(\varepsilon,\tau,N) = \inf_{\varphi}\delta_1(\varphi;\varepsilon,\tau,N), \tag{3.12}$$

where the infimum is over all φ satisfying (2.17). Find a cutoff function φ satisfying (2.17) which minimizes (3.12).

From (2.40) and (3.9) we get immediately

$$\delta_1(\varphi;\varepsilon,\tau,N) \le \delta_\infty(\varphi;\varepsilon,\tau,N). \tag{3.13}$$

Hence, the upper bound from Theorem 3.2 holds for $\delta_1(\varepsilon,\tau,N)$ as well. But one can improve this estimate as follows

Theorem 3.6. *Let $N\in\mathbb{N}$, $0<\varepsilon\le e^{-1}$ and $\tau\ge 1$. Then there exist absolute constants $c^\#, c^*>0$ such that for $N\ge \ln(1/\varepsilon)+c^*$ we have*

$$\delta_1(\varepsilon,\tau,N) \le \frac{c^\#\ln(1/\varepsilon)}{\tau N}. \tag{3.14}$$

Proof. From Theorem 3.1 we get

$$\frac{1}{2}\int\limits_{-1}^{\cos\delta} |\mathcal{K}_N(u)|\,du \le \frac{1}{2}\int\limits_{\delta}^{\pi} |\mathcal{K}_N(\cos\theta)|\theta\,d\theta \le \frac{c_0\left((1+\tau)N\right)^2}{2}\int\limits_{\delta}^{\infty}\left(\frac{c_1 k}{\tau N\theta}\right)^k \theta\,d\theta \tag{3.15}$$

$$= \frac{c_0 c_1^2 k^2(1+\tau)^2}{2\tau^2}\int\limits_{\frac{\tau N\delta}{c_1 k}}^{\infty} v^{-k+1}\,dv = \frac{c_0 c_1^2 k^2(1+\tau)^2}{2(k-2)\tau^2}\left(\frac{c_1 k}{\tau N\delta}\right)^{k-2}.$$

Let $\kappa\ge 4$ be such that $4c_0c_1^2 u e^{-u}\le 1$ for $u\ge\kappa$. Set $k=\lceil\ln(1/\varepsilon)+\kappa\rceil$ and $\delta = e^2 c_1 k/(\tau N)$. Then from (3.15), $\tau\ge 1$ and $k\ge\kappa\ge 4$ we get

$$\frac{1}{2}\int\limits_{-1}^{\cos\delta} |\mathcal{K}_N(u)|\,du \le 4c_0c_1^2 k e^{-k}e^{-k+4} \le e^{-\ln(1/\varepsilon)}e^{-\kappa+4} \le \varepsilon. \tag{3.16}$$

Now (3.16) proves the theorem with $c^\# = e^2c_1(\kappa+1)$ and $c^* = \kappa+1$ (which implies $N>k$). □

Note that for a fixed ε the upper bound for $\delta_1(\varepsilon,\tau,N)$ in (3.14) with the increase of N becomes smaller than the lower bound for $\delta_\infty(\varepsilon,\tau,N)$ in Theorem 3.2. This fact justifies the replacement of criterion (2.40) from Theorem 2.4 by criterion (3.9) for practical application. Note that the product $N\delta_1(\varepsilon,\tau,N)$ is bounded from above by a quantity depending on ε and τ but not on N. This means that the complexity of (2.30) will not depend on N and we can use $\Phi_{N,\delta}$ for very high degrees N.

Selection of $\boldsymbol{\varphi}$. For fixed φ, ε, τ and N it is easy to write a code for approximate computation of $\delta_1(\varphi;\varepsilon,\tau,N)$ from (3.9) and thus to compare the values of δ_1 for different φ's. Although such approach will not lead to a solution of Problem 4, it guided us in selecting a cutoff function φ for our purposes.

We work with φ satisfying (2.17), which for t in the interval $[1,1+\tau]$ are given by

$$\varphi(t)=\kappa^{-1}\int\limits_{(t-1)/\tau}^{1} e^{b\sqrt{v(1-v)}}\,dv,\quad \kappa=\int\limits_{0}^{1} e^{b\sqrt{v(1-v)}}\,dv,\ b>0. \tag{3.17}$$

In (3.17) b is a parameter, which for $4<\log_{10}(1/\varepsilon)<11$ and $\tau\ge 1$ is given by

$$b=4.8\log_{10}(1/\varepsilon)+3.4-0.2\min\{\tau,3\}. \tag{3.18}$$

The graph in the interval $[0,0.009]$ of the kernel $\mathcal{K}_{1000}\circ\cos$ generated by φ defined in (3.17)–(3.18) with $\tau=4$ and $\varepsilon=10^{-7}$ is given in Figure 1, while Table 1 contains its local extrema and their locations on the same interval. Figure 2 gives the semi-log graph of the absolute value of the same kernel on the bigger interval $[0,0.018]$.

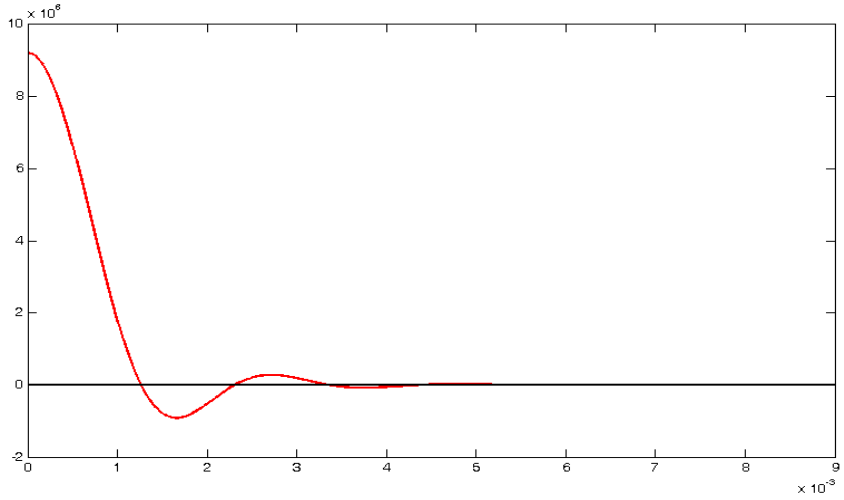

FIGURE 1. Graph of $\mathcal{K}_{1000}\circ\cos$ in $[0,0.009]$ for $\tau=4$ and $\varepsilon=10^{-7}$

The computed values of $\delta_1(\varphi;\varepsilon,\tau,N)$ for φ from (3.17) with b from (3.18) can be very well approximated by the expression

$$\delta_1(\varepsilon,\tau,N)\approx\frac{\tilde{c}\ln(1/\varepsilon)}{\tau N} \tag{3.19}$$

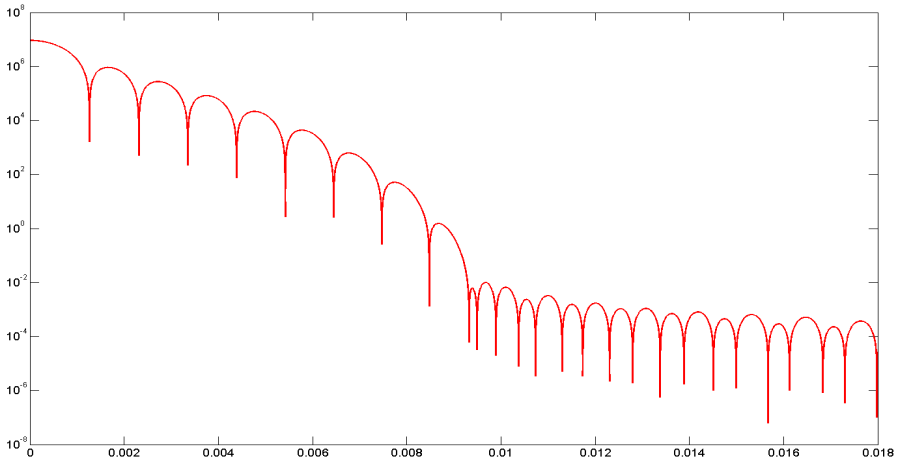

FIGURE 2. Semi-log graph of $|\mathcal{K}_{1000}| \circ \cos$ in $[0, 0.018]$ for $\tau = 4$ and $\varepsilon = 10^{-7}$

Abscissa	Value	Abscissa	Value
0	$9.2049 \cdot 10^{6}$	$5.7680 \cdot 10^{-3}$	$-4.3761 \cdot 10^{3}$
$1.6575 \cdot 10^{-3}$	$-9.1850 \cdot 10^{5}$	$6.7632 \cdot 10^{-3}$	$6.2170 \cdot 10^{2}$
$2.7150 \cdot 10^{-3}$	$2.7573 \cdot 10^{5}$	$7.7384 \cdot 10^{-3}$	$-5.1301 \cdot 10^{1}$
$3.7442 \cdot 10^{-3}$	$-8.3107 \cdot 10^{4}$	$8.6708 \cdot 10^{-3}$	$1.5374 \cdot 10^{0}$
$4.7614 \cdot 10^{-3}$	$2.1568 \cdot 10^{4}$	–	–

TABLE 1. The extrema of $\mathcal{K}_{1000} \circ \cos$ and their abscissas in $[0, 0.009]$ for $\tau = 4$ and $\varepsilon = 10^{-7}$

with an appropriate constant $\tilde{c}$, which corresponds to the upper limit from (3.14). The values of $\delta_1(\varphi; \varepsilon, \tau, 1000)$ for some ε and τ are given in Table 2.

$\tau \backslash \varepsilon$	10^{-5}	10^{-6}	10^{-7}	10^{-8}	10^{-9}	10^{-10}
1	0.0278	0.0325	0.0372	0.0419	0.0468	0.0515
2	0.0137	0.0162	0.0185	0.0209	0.0232	0.0257
3	0.00917	0.0107	0.0123	0.0138	0.0155	0.0171
4	0.00685	0.00802	0.00919	0.0103	0.0116	0.0128

TABLE 2. Values of $\delta_1(\varphi; \varepsilon, \tau, 1000)$ for φ from (3.17)–(3.18)

The entries in the Table 2 support the dependance of δ_1 on ε and τ as suggested in (3.19) with a value of $\tilde{c}$ between 2.22 and 2.42. Moreover, our computations show that the quantity $N\delta_1(\varphi; \varepsilon, \tau, N)$ is practically a constant for $100 \leq N \leq 10\,000$ for every fixed ε and τ in the specified range.

3.3. **Accurate kernel evaluation.** The next step in developing our algorithm is the accurate and fast evaluation of $\mathcal{K}_N(x \cdot y)$ for given $x, y \in \mathbb{S}^2$, which is a nontrivial task.

For every $u \in [-1,1]$ one can evaluate $\mathcal{K}_N(u)$ using, for instance, the downward Clenshaw recurrence formula. It employs the Legendre recurrence relation

$$(n+1)P_{n+1}(u) = (2n+1)uP_n(u) - nP_{n-1}(u),\ n \geq 0; \quad P_0(u) = 1,\ P_{-1}(u) = 0.$$

This algorithm is numerically stable and fast since it requires $O(N)$ operations.

The straightforward calculation of $\mathcal{K}_N(x \cdot y)$, where $u = x \cdot y$ is obtained via (2.5) and $\mathcal{K}_N(u)$ is computed by the Clenshaw summation, looses accuracy when x is close to y that is exactly the case we are interesting in. In order to improve the accuracy by several significant digits we perform the calculations as follows:

(i) We compute the spherical distance ρ between $x = (\theta, \lambda)$ and $y = (\theta', \lambda')$ via the Haversine Law of Spherical Trigonometry

$$\sin^2 \frac{\rho}{2} = \sin^2 \frac{\theta' - \theta}{2} + \sin\theta' \sin\theta \sin^2 \frac{\lambda' - \lambda}{2}. \tag{3.20}$$

(ii) We compute $\mathcal{K}_N(x \cdot y) = (\mathcal{K}_N \circ \cos)(\rho)$ via an approximation of $\mathcal{K}_N \circ \cos$.

The Haversine Law (3.20) is well-conditioned for computation of ρ close to 0 and the round-off error is smaller when compared with the Spherical Law of Cosines (2.5). This fact has been known since the XIX century. The haversine function is defined by $\operatorname{hav}\rho := (1 - \cos\rho)/2 = \sin^2(\rho/2)$; we have used the last form in (3.20).

The advantage of using the trigonometric polynomial $\mathcal{K}_N \circ \cos$ in step (ii) over the algebraic polynomial $\mathcal{K}_N$ stems from the fact that the derivative of $\mathcal{K}_N \circ \cos$ near the origin is cN times smaller than the derivative of $\mathcal{K}_N$ near 1.

In order to get fast and accurate evaluation of $(\mathcal{K}_N \circ \cos)(\rho)$ for $\rho \in [0, \delta]$ we take the equally spaced points $t_r = \delta r/R$ for $r = -s, -s+1, \ldots, R+s$ and determine $t_r^* = \arccos(\cos t_r)$. Note that in general $t_r^* \neq t_r$ because of the machine arithmetic, while $\cos t_r^*$ and $\cos t_r$ coincide as double precision numbers. Then $\mathcal{K}_N(u_r)$, determined for $u_r = \cos t_r = \cos t_r^*$ via the Clenshaw summation, is a good approximation to $(\mathcal{K}_N \circ \cos)(t_r^*)$. Thus we have the values of $\mathcal{K}_N \circ \cos$ at the points t_r^*, which are close to equally spaced but not equally spaced. Now $(\mathcal{K}_N \circ \cos)(\rho)$ is computed by Lagrange interpolation of $\mathcal{K}_N \circ \cos$ with nodes t_r^*, $r = m-s, m-s+1, \ldots, m+s+1$, where $m = \lfloor \rho R/\delta \rfloor$. The Lagrange polynomial is of degree $2s+1$.

The choice of R and s depends on the targeted relative error ε and the degree $N_\tau - 1$ of $\mathcal{K}_N \circ \cos$. Our experiments showed that for $\varepsilon \geq 10^{-10}$ and $N_\tau \leq 20\,000$ one can take $R = 2\,000$ and $s = 1$ or $s = 2$. The numbers $\mathcal{K}_N(u_r)$ are computed in $O(NR)$ operations and stored at the initial stage of the program. At the later stages the evaluation of $(\mathcal{K}_N \circ \cos)(\rho)$ requires only $O(s)$ operations. Of course, the third degree Lagrange interpolation, i.e. $s = 1$, is faster but less accurate than the fifth degree Lagrange interpolation for $s = 2$.

The graph of the kernel $\mathcal{K}_N \circ \cos$ in $[0, \delta]$ as well its extrema and their location in this interval are given in Figures 1 and 2 and Table 1 in §3.2.

3.4. **Nodes and cubatures.** The following lemma gives a simple method for constructing cubatures on $\mathbb{S}^2$ from one-dimensional quadratures. These simple cubatures are very attractive since they are exact for high degree spherical polynomials and their nodes and weights can be computed easily to very high precision. They also demonstrate the advantage of the regular grids defined in §2.1 over other grids such as HEALPix.

Lemma 3.7. *Let $K, L \geq 1$ and assume that the quadrature*

$$\frac{1}{2}\int_{-1}^{1} f(t)\,dt \sim \sum_{k=0}^{K} v_k f(u_k), \tag{3.21}$$

with $u_k \in [-1,1]$ is exact for all algebraic polynomials of degree $K_1 - 1$ and the quadrature

$$\frac{1}{2\pi}\int_{0}^{2\pi} g(t)\,dt \sim \sum_{\ell=0}^{L-1} \bar{v}_\ell g(\lambda_\ell), \tag{3.22}$$

with $\lambda_\ell \in [0, 2\pi)$ is exact for all trigonometric polynomials of degree $L_1 - 1$. Then the cubature

$$\frac{1}{4\pi}\int_{\mathbb{S}^2} F(y)\,d\sigma(y) \sim \sum_{k=0}^{K}\sum_{\ell=0}^{L-1} v_k \bar{v}_\ell F(\arccos(u_k), \lambda_\ell) \tag{3.23}$$

is exact for all spherical polynomials of degree $M - 1$ with $M = \min\{K_1, L_1\}$.

The lemma is immediate from the form of the basis of $\mathcal{H}_n$ given in (2.6) (with the variables separated) and the form of the measure $d\sigma$ given in (2.10).

Note that if $u_k = 1$, then all nodes $(\arccos(u_k), \lambda_\ell) = (0, \lambda_\ell)$ coincide with the North Pole and the cubature weight associated with this node is $v_k = \sum_{\ell=0}^{L-1} v_k \bar{v}_\ell$. A similar modification is made if $u_k = -1$, i.e the node coincides with the South Pole.

The case of quadrature (3.22) is quite simple, the best choice is the rectangular quadrature

$$\frac{1}{2\pi}\int_{0}^{2\pi} g(t)\,dt \sim \sum_{\ell=0}^{L-1} \frac{1}{L} g(\lambda_\ell), \quad \lambda_\ell = \frac{2\pi}{L}\ell,\ \ell = 0, \ldots, L-1, \tag{3.24}$$

which is exact for trigonometric polynomials of degree $L - 1$.

The algebraic quadrature formulas (3.21) with nodes $\{\cos\theta_k^{(i)}\}$, $i = 1, 2, 3$, from §2.1 are given in the following three lemmas.

Lemma 3.8. *For given $K \geq 1$ denote by $u_k^{(1)} = \cos\theta_k^{(1)}$, $\theta_k^{(1)} = \pi k/K$, $k = 0, 1, \ldots, K$, the points of extrema of the Chebyshev polynomial T_K. If the weights $\{v_k^{(1)}\}$ are defined by*

$$v_0^{(1)} = v_K^{(1)} := \frac{1}{2K(2R+1)}, \tag{3.25}$$

$$v_k^{(1)} := \frac{1}{K}\left(\frac{1}{2R+1} + 4\sum_{r=1}^{R} \frac{\sin^2 r\theta_k^{(1)}}{4r^2 - 1}\right), \quad k = 1, \ldots, K-1,$$

where $R = \lfloor (K-1)/2 \rfloor$, then the quadrature

$$\frac{1}{2}\int_{-1}^{1} f(t)\,dt \sim \sum_{k=0}^{K} v_k^{(1)} f(u_k^{(1)}), \tag{3.26}$$

is exact for all algebraic polynomials of degree $2\lfloor (K+1)/2 \rfloor - 1 \geq K - 1$.

Lemma 3.9. *Given $K \geq 1$ denote by $u_k^{(2)} = \cos\theta_k^{(2)}$, $\theta_k^{(2)} = \pi(2k-1)/(2K)$, $k = 1, \dots, K$, the zeros of the Chebyshev polynomial T_K. If the weights $\{v_k^{(2)}\}$ are defined by*

$$v_k^{(2)} := \frac{1}{K}\left(\frac{1}{2R+1} + 4\sum_{r=1}^{R}\frac{\sin^2 r\theta_k^{(2)}}{4r^2-1}\right), \quad k = 1, \dots, K, \tag{3.27}$$

where $R = \lfloor (K-1)/2 \rfloor$, then the quadrature

$$\frac{1}{2}\int_{-1}^{1} f(t)\,dt \sim \sum_{k=1}^{K} v_k^{(2)} f(u_k^{(2)}), \tag{3.28}$$

is exact for all algebraic polynomials of degree $2\lfloor (K+1)/2 \rfloor - 1 \geq K-1$.

Quadrature (3.26) is usually known as the Clenshaw–Curtis quadrature [1] or Fejér's second quadrature. (In [7, 8] Fejér gave the values of $v_k^{(1)}$ under the assumption that $f(-1) = f(1) = 0$.) Quadrature (3.28) is usually known as Fejér's first quadrature [7, 8]. The weight expressions (3.25), (3.27) deviate from the standard ones, but we prefer these forms because they underline the weights' positivity.

Lemma 3.10. *For $K \geq 1$ denote by $u_k^{(3)} = \cos\theta_k^{(3)}$, $\theta_k^{(3)} \in (0, \pi)$, $k = 1, \dots, K$, the zeros of the Legendre polynomial P_K. If the weights $\{v_k^{(3)}\}$ are defined by*

$$v_k^{(3)} := \left(P_K'(\cos\theta_k^{(3)})\sin\theta_k^{(3)}\right)^{-2}, \quad k = 1, \dots, K, \tag{3.29}$$

then the Gaussian quadrature

$$\frac{1}{2}\int_{-1}^{1} f(t)\,dt \sim \sum_{k=1}^{K} v_k^{(3)} f(u_k^{(3)}), \tag{3.30}$$

is exact for all algebraic polynomials of degree $2K-1$.

To compute the knots $u_k^{(3)} = \cos\theta_k^{(3)}$ and weights $v_k^{(3)}$ of the Gaussian quadrature we use the MATLAB function `legpts` from `Chebfun` software system by Trefethen et all [27]. It utilizes a fast and accurate algorithm from Glaser, Liu and Rokhlin [10], which shows very good results for quadratures with up to a million knots.

Applying (3.24) and Lemmas 3.8–3.10 in Lemma 3.7 we get

Theorem 3.11. *Let $M \geq 1$ and assume that $\mathcal{X}^{(i)}$, $i = 1, 2, 3$, is one of the regular grids from §2.1 with $K, L \geq 1$ satisfying the conditions*

$$M \leq L, \qquad M \leq \begin{cases} 2\lfloor (K+1)/2 \rfloor, & i = 1, 2; \\ 2K, & i = 3. \end{cases} \tag{3.31}$$

For $\xi = (\theta_k^{(i)}, \lambda_\ell^{(i)}) \in \mathcal{X}^{(i)}$ set $w_\xi^{(i)} = v_k^{(i)} L^{-1}$. Then the cubature

$$\frac{1}{4\pi}\int_{\mathbb{S}^2} F(y)\,d\sigma(y) \sim \sum_{\xi \in \mathcal{X}^{(i)}} w_\xi^{(i)} F(\xi) \tag{3.32}$$

is exact for all spherical polynomials of degree $M-1$.

In other words, if $K \geq M$ and $L \geq M$, then we have a cubature satisfying (2.27) with nodes at the regular grid points from (2.1) or (2.2). In a number of applications we have $L \approx 2K$ because at the equator the mesh size is $2\pi/L$ in the longitude direction and π/K in the latitude direction. For the grid points (2.3) the condition $K \geq M$ may be relaxed to $K \geq M/2$.

Our next step is to show that the cubatures from Theorem 3.11 satisfy (2.28). To this end for any finite set $\mathcal{X} \subset \mathbb{S}^2$ we define the Voronoi cells Ω_ξ, $\xi \in \mathcal{X}$, by

$$\Omega_\xi = \{x \in \mathbb{S}^2 \ : \rho(x,\xi) \leq \rho(x,\eta) \ \forall \eta \in \mathcal{X}\},$$

i.e. Ω_ξ consists of all points from the sphere, which are closer to ξ than to any other point from $\mathcal{X}$. Note that every cell is a convex spherical polygon. The set of all Voronoi cells forms the Voronoi tessellation of $\mathbb{S}^2$. Thus $\cup_{\xi\in\mathcal{X}}\Omega_\xi = \mathbb{S}^2$ and the interiors of any two different cells are disjoint.

For every $\xi \in \mathcal{X}$ the set A_ξ from (2.28) is defined as the interior of Ω_ξ plus some points from its boundary so that $\{A_\xi\}_{\xi\in\mathcal{X}}$ forms a disjoint partition of $\mathbb{S}^2$. Now it is easy to prove

Theorem 3.12. *Under the hypothesis of Theorem 3.11 the cubature* (3.32) *satisfies* (2.28).

Proof. For the Gaussian quadrature ($i = 3$) it is well known that uniformly

$$\theta^{(3)}_{k+1} - \theta^{(3)}_k \sim K^{-1}, \ k = 1, 2, \ldots, K-1, \quad \theta^{(3)}_1 \sim K^{-1}, \quad \pi - \theta^{(3)}_K \sim K^{-1}. \tag{3.33}$$

Using also $\lambda^{(3)}_{\ell+1} - \lambda^{(3)}_\ell = 2\pi L^{-1}$ we get $A_\xi \subset B(\xi, r)$ with $r = O(\max\{K^{-1}, L^{-1}\}) = O(M^{-1})$ and $\sigma(A_\xi) \sim K^{-1}L^{-1}\sin\theta^{(3)}_k$. The weights $v^{(3)}_k$ are positive and satisfy uniformly (see e.g. [21])

$$v^{(3)}_k \sim K^{-1}\sin\theta^{(3)}_k, \quad k = 1, 2, \ldots, K, \tag{3.34}$$

which implies $w^{(3)}_\xi \leq c_2\sigma(A_\xi)$ and proves the theorem in the case $i = 3$.

If $i = 1$ or $i = 2$ we have estimates similar to (3.33) and (3.34). Estimate (3.34) follows from (3.25) and (3.27), and (3.33) follows from (2.1) and (2.2). The only exceptions are the two poles ($k = 0$ and $k = K$) in the case $i = 1$. If ξ is any of them, we have $\sigma(\Omega_\xi) \sim K^{-2}$ and $w^{(1)}_\xi = K^{-1}(2\lfloor (K-1)/2\rfloor + 1)^{-1}$. This completes the proof. □

Theorem 3.11 and Theorem 3.12 show that cubatures (3.32) satisfy (2.27) and (2.28) under the assumptions (3.31). Consequently, if (2.34) is verified, then the operators from (2.29) and (2.30) satisfy Theorem 2.3 and Theorem 2.4, respectively, for each of the cubatures (3.32).

We now turn our attention to the problem for determining the nodes $\xi = (\theta, \lambda) \in \mathcal{X}^{(i)}$, which satisfy $\rho(x,\xi) \leq \delta$ for given $x = (\theta', \lambda') \in \mathbb{S}^2$ and $\delta \in (0, \pi/2]$. From the Law of Sines in spherical trigonometry we conclude that for $\delta \leq \theta' \leq \pi - \delta$ it suffices to have

$$(\theta, \lambda) \in [\theta' - \delta, \theta' + \delta] \times [\lambda' - \phi, \lambda' + \phi], \quad \phi = \arcsin(\sin\delta/\sin\theta'). \tag{3.35}$$

For $0 \leq \theta' < \delta$ (3.35) can be replaced by $(\theta, \lambda) \in [0, \theta' + \delta] \times [0, 2\pi)$ and for $\pi - \delta < \theta' \leq \pi$ by $(\theta, \lambda) \in [\theta' - \delta, \pi] \times [0, 2\pi)$. It is easy to create code which determines quickly the indices of the grid points $\xi = (\theta_k, \lambda_\ell)$ satisfying (3.35). Observe that approximately $\pi/4$ of the grid points obeying (3.35) satisfy $\rho(x,\xi) \leq \delta$. Thus, if

the kernel is evaluated for all grid points satisfying (3.35), then the extra work of 27.4% could be fully compensated by not performing the verification $\rho(x,\xi)\le\delta$.

The number of points from $\mathcal{X}^{(i)}$, $i=1,2,3$, satisfying (3.35) is approximately

$$\nu=\frac{2KL\delta^2}{\pi^2\sin\theta'}. \tag{3.36}$$

Thus the number of terms in (2.30) increases from $O(KL\delta^2)$ for points at the equator to $O(KL\delta)$ for points near the poles. This drawback of our method can easily be overcome as shown in §3.5.

3.5. **Computations near the poles.** In order to evaluate $\Phi_{N,\delta}f(x)$ at points $x=(\theta',\lambda')$ with latitudes between 45° North and 45° South, i.e. $\pi/4\le\theta'\le 3\pi/4$, we apply the method as explained so far. For the remaining points from the two 45° caps centered at the poles we apply the change of variables $T(x)=\tilde{x}$ given by

$$(x_1,x_2,x_3)=(\tilde{x}_1,\tilde{x}_3,-\tilde{x}_2) \tag{3.37}$$

(T is a 90° rotation about the x-axis) or in spherical coordinates

$$(\sin\theta\cos\lambda,\sin\theta\sin\lambda,\cos\theta)=(\sin\tilde{\theta}\cos\tilde{\lambda},\cos\tilde{\theta},-\sin\tilde{\theta}\sin\tilde{\lambda}).$$

In the new coordinate system the above spherical caps appear as 45° caps centered at the points $(\pi/2,\pi/2)$ and $(\pi/2,3\pi/2)$, which are on the new equator. In order to apply the same operators Φ_N and $\Phi_{N,\delta}$ we need the values of the spherical polynomial to be computed at the regular grid points with respect to the new coordinate system, i.e. the values at the images $T^{-1}(\xi)$, $\xi\in\mathcal{X}$, of these grid points under the mapping T^{-1}, which is inverse to (3.37). Note that each of the spaces $\mathcal{H}_n$, $n=0,1,2,\dots$, is invariant under the rotation (3.37).

A simple and efficient method for rotation of spherical harmonic expansions is developed in [9]. This method has cubic complexity with respect to the polynomial degree.

Using this approach we essentially improve the computational speed for points near the poles. Now in the worst case scenario the evaluation of $\Phi_{N,\delta}f(x)$ requires a factor of $\sqrt{2}$ more points than the points used when x is on the equator. Another positive feature is the reduction of the total number of nodes where we have to pre-compute the polynomial values. The reduction is by approximately 25% and is due to the fact that the grid points, which are denser near the poles, are replaced by new points with "equatorial" density.

In the following table we give *the average number of nodes in the δ-neighborhood of a point*, i.e. the average number of summands in (2.30), when φ is defined by (3.17)–(3.18). The computations were performed for $N=1000$, but, as it was pointed out in §3.2, the average number of nodes is practically independent of the polynomial degree N. The nodes in Table 3 are from the regular grid $\mathcal{X}^{(3)}$ with $K=\lceil(1+\tau/2)N\rceil$ and $L=\lceil(2+\tau)N\rceil$. According to Theorem 3.11 the cubature based on these nodes is exact for spherical polynomials of degree $M-1$ with $M=\lceil(2+\tau)N\rceil$.

In the case when the nodal set is either $\mathcal{X}^{(1)}$ or $\mathcal{X}^{(2)}$ with $K=\lceil(2+\tau)N\rceil$ the average number of nodes is twice bigger than the entries of Table 3.

3.6. **Optimal selection of parameters.** The data from Table 3 brings to the table the following problem:

$\tau\backslash\varepsilon$	10^{-5}	10^{-6}	10^{-7}	10^{-8}	10^{-9}	10^{-10}
1	612	838	1091	1380	1735	2095
2	263	371	478	617	754	929
3	189	255	327	414	530	640
4	149	203	265	336	421	522

TABLE 3. The average number of nodes from $\mathcal{X}^{(3)}$ in the δ-neighborhood for δ's given in Table 2.

Suppose a spherical polynomial of degree N is given by its values at, say, the $M/2 \times M$ regular grid points (2.3). Choose τ subject to (2.34) so that the number of summands in (2.30) is minimal.

To be more specific, let, say, $N = 1000$, $M = 6000$, $\varepsilon = 10^{-8}$ and $\delta = \delta_1(\varphi; \varepsilon, \tau, N)$ as in §3.2. Consider the following two selections of τ:

(i) $\tau = 4$ in the definition of φ and we make the computations using $\delta = \delta_1(\varphi; \varepsilon, 4, N)$ and the $3\,000 \times 6\,000$ grid ($M = 6\,000$);
(ii) $\tau = 1$ in the definition of φ and we make the computations using $\delta = \delta_1(\varphi; \varepsilon, 1, N)$ and the $1\,500 \times 3\,000$ sub-grid ($M = 3\,000$) of the grid in (i). Of course, we can use a larger sub-grid, but this will lead only to higher number of terms.

The question is, in which case the cap $\{y \in \mathbb{S}^2 : \rho(x, y) \le \delta\}$ will contain less points ξ from the respective grid.

Note that (2.34) is satisfied as equality in both cases. This makes us define $M := \lceil N(2+\tau) \rceil$ which is the best choice for the grid parameter. The number of grid points in the δ-neighborhood of a point is a constant multiple of $(M\delta)^2 = ((2+\tau)N\delta)^2$.

Without going into details we would like to mention the asymptotic equality

$$\delta_1(\varphi; \varepsilon, \tau, N) \approx \frac{C(\varepsilon, \tau)}{\tau N} \tag{3.38}$$

valid for a fixed φ. In fact, $C(\varepsilon, \tau)$ in (3.38) is a slowly varying function of ε and $\tau \ge 1$ (e.g. $C(\varepsilon, \tau) = c_1 \ln(1/\varepsilon) + c_2 \ln(1 + 1/\tau)$, cf. (3.19)), which has a limit as $\tau \to \infty$.

Thus the number of summands in (2.30) is proportional to $(1 + 2\tau^{-1})^2$ (cf. Table 3), which is a decreasing function of τ. In particular, this result implies that the smallest number of terms for given N and M will be achieved for the largest possible τ in (2.34), in other words

we cannot gain speed by using sub-grids.

Going back to our example, in case (i) we have approximately 4 times less terms than in case (ii). Thus, the computational speed in case (i) will be 4 times higher than in case (ii). But, one should not forget that the initial work for evaluating the polynomial in the grid points is 4 times bigger in case (i) than in case (ii).

3.7. **The algorithm.** Based on the ideas from §2 and §3 we propose the following algorithm for solving Problem 3 with input N, ε_0 and $Y_N(\xi)$, $\xi \in \mathcal{X}^{(i)}$ for one of $i = 1, 2, 3$:

(1) Using (3.25), (3.27) or (3.29) determine the weights $w_\xi^{(i)}$, $i = 1, 2, 3$, of the cubature (3.32) according to the type i of the grid $\mathcal{X}^{(i)}$ from §2.1.
(2) Determine the largest possible M for the cubature.
(3) For the given M, N determine the largest possible τ satisfying (2.34).
(4) Determine $\|Y_N\|_{\ell^\infty(\mathcal{X})}$ and then ε from (3.1).
(5) For φ given by (3.17)–(3.18) determine $\varphi(n/N)$.
(6) Determine $\delta = \delta_1(\varphi; \varepsilon, \tau, N)$ from (3.9).
(7) For φ and δ from Steps 5–6 compute $\mathcal{K}_N(\cos t_r^*)$, $r = -s, -s+1, \dots, R+s$ (see §3.3).
(8) For every $x \in \mathcal{Z}$ compute the approximate value $\Phi_{N,\delta} Y_N(x)$ of $Y_N(x)$ using (2.30) with $f = Y_N$, where $\mathcal{K}_N(x \cdot \xi) = (\mathcal{K}_N \circ \cos)(\rho)$ is determined as in §3.3 with ρ determined from (3.20).

If the improvement described in §3.5 is applied, then in Step 8 one verifies for every $x \in \mathcal{Z}$ in advance to which of the three domains $\{\theta < \pi/4\}$, $\{\pi/4 \le \theta \le 3\pi/4\}$ and $\{\theta > 3\pi/4\}$ it belongs and in two of the three cases rotation (3.37) is applied before computing the approximation in (2.30).

We next determine the complexity of all steps in the typical case $K = O(N)$, $L = O(N)$. Step 1 requires $O(N \ln N)$ operations when FFT is used for computing $v_k^{(i)}$. Step 4 requires $O(N^2)$ operations. The values $\varphi(n/N)$ in Step 5 can be computed in $O(N)$ operations and the computation of δ in Step 6 can be done with good precision with $O(N^2)$ operations. Step 7 requites $O(NR)$ operations. The total complexity of the preparatory Steps 1–7 is $O(N^2)$ without counting the operations necessary to compute $Y_N(\xi)$, $\xi \in \mathcal{X}^{(i)}$, or the time to read them from the disk. As explained in the introduction, the stable algorithms for computing $Y_N(\xi)$, $\xi \in \mathcal{X}^{(i)}$, require $O(N^3)$ (direct computation with straightforward separation of variables) or $O(N^2 \ln N)$(Tygert approximate algorithm) operations.

From inequalities (3.14) and (3.3) we get that the approximate evaluation of Y_N by (2.30) at a single point requires $O(\ln^2(1/\varepsilon_0))$ operations if δ is determined by criterion (3.9) and $O(\ln^2(N^2/\varepsilon_0))$ operations if criterion (2.40) is applied.

4. Generalizations and applications

4.1. **Generalization to higher dimensions.** Let $\mathbb{S}^d$ ($d \ge 1$) be the unit sphere in $\mathbb{R}^{d+1}$ and denote by $\mathcal{H}_n^d$, $n \ge 0$, the space of all spherical harmonics of degree n on $\mathbb{S}^d$. It is well known [25, p. 140] that $\dim \mathcal{H}_n^d = \frac{(2n+d-1)\Gamma(n+d-1)}{\Gamma(d)\Gamma(n+1)}$ for $n \ge 1$ and $\dim \mathcal{H}_0^d = 1$.

As is well known [25] the orthogonal projector $\mathrm{Proj}_{\mathcal{H}_n^d} : L^2(\mathbb{S}^d) \to \mathcal{H}_n^d$ has the representation (a generalization of (2.11))

$$(\mathrm{Proj}_{\mathcal{H}_n^d} f)(x) = \frac{1}{\omega_d} \int_{\mathbb{S}^d} \frac{n+\kappa}{\kappa} C_n^\kappa(x \cdot y) f(y) d\sigma(y), \tag{4.1}$$

where σ is the standard Lebesgue measure on $\mathbb{S}^d$, $\kappa := \frac{d-1}{2}$, $\omega_d := \int_{\mathbb{S}^d} 1 d\sigma = \frac{2\pi^{\kappa+1}}{\Gamma(\kappa+1)}$, and $x \cdot y$ stands for the inner product of $x, y \in \mathbb{S}^d$. Here C_n^κ is the Gegenbauer polynomial of degree n normalized with $C_n^\kappa(1) = \binom{n+2\kappa-1}{n}$ [6, p. 174].

Using the relationship between Gegenbauer and Jacobi polynomials [26, (4.7.1)]

$$C_n^\kappa(u) = \frac{\Gamma(\kappa+1/2)}{\Gamma(2\kappa)} \frac{\Gamma(n+2\kappa)}{\Gamma(n+\kappa+1/2)} P_n^{(\kappa-1/2, \kappa-1/2)}(u)$$

we obtain the following generalization of (2.16)

$$\mathcal{K}_N(u) = \sum_{n=0}^{\infty} \varphi\Big(\frac{n}{N}\Big) \frac{(n+\kappa)\Gamma(\kappa+1/2)\Gamma(n+2\kappa)}{\kappa\Gamma(2\kappa)\Gamma(n+\kappa+1/2)} P_n^{(\kappa-1/2,\kappa-1/2)}(u). \tag{4.2}$$

In dimension $d = 1$ one has after passing to the limit in (4.1) and (4.2) as $\kappa \to 0$ (here $F = f \circ \cos$)

$$(\mathrm{Proj}_{\mathcal{H}_n^1} F)(x) = \frac{1}{2\pi} \int_0^{2\pi} (2 - \delta_{n,0}) \cos n(x-\theta) F(\theta) d\theta,$$

$$\mathcal{K}_N(u) = \sum_{n=0}^{\infty} \varphi\Big(\frac{n}{N}\Big)(2 - \delta_{n,0}) T_n(u),$$

where T_n is the n-th degree Chebyshev polynomial and $\delta_{n,m}$ is the Kronecker delta.

The point is that in the general case all necessary ingredients are either known, e.g. the generalization of the sub-exponential decay of $\mathcal{K}_N$ in Theorem 2.2 is established in [12, Theorem 5.1], or can be derived following the same route as when $d = 2$. Let us only mention that estimate (3.14) remains true. Hence, the number of summands in (2.30) becomes $O(\ln^d(1/\varepsilon_0))$.

Finally, let us point out that in the case $d = 1$ our method serves as an algorithm for fast evaluation of trigonometric polynomials at scattered points.

4.2. **Working with grids of wider mesh size.** There are two groups of conditions important to our theory: (a) inequalities (3.31) connecting K and L with M, and (b) $\deg Y_N \le N$ and inequality (2.34) connecting M with N. The first group can be consider as a simple definition of the term "spherical degree of exactness M". For simplicity in this subsection we consider the case of "Gaussian" nodes $\mathcal{X}^{(3)}$ (with $L = 2K = M$), so the distance at the equator between the nodes is $2\pi/M$ in both latitude (approximately) and longitude directions.

We now turn our attention to the conditions from group (b). Let $\widetilde{N} = \deg Y_N$ be the exact degree of the polynomial to be evaluated. The condition $\widetilde{N} \le N$ is implicitly part of our theory, however, in applications one can choose in (2.16) $N < \widetilde{N}$. Similarly, condition (2.34) was essentially used in establishing (2.35) in Theorem 2.3 and (2.42) in Theorem 2.4, which enable us to claim that the error of approximation does not exceed ε_0. In the typical case $\tau = 1$, however, inequality (2.34) implies $M \ge 3N$, i.e. the nodes are at least 1.5 times denser (linearly) than the the sampling interval for the Nyquist frequency π/N for Nth degree polynomials. Therefore, the fundamental question here is:

Can one utilize successfully the truncated operators from (2.30) whenever (A) $N < \widetilde{N}$ and/or (B) $M < (2+\tau)N$?

We would like to emphasize that we are interested in significant reductions of the sizes of N and M above. A small percentage reductions of N and M are always possible since the cutoff coefficients $\varphi(n/N)$ are very close to 1 when n is close to N and very small when n is close to N_τ. Also the trivial positive answer of question (B) that (2.30) is applicable for $M > 2N$ (with $\bar{\tau} = MN^{-1} - 2$) is not very satisfactory. Of course, one will be covered by the theory but, as explained in §3.6, decreasing τ below 1 reduces significantly the speed of the algorithm.

One can write explicitly the errors which conditions (A) and (B) bring in property (2.35). Effects of such type are often called "aliasing". These questions can also be explored numerically when taking ε smaller than the aliasing error. One of the conclusions from our experiments in Example 1 in §5 is that condition (A) is more damaging to the error than condition (B) for polynomials with "large" high degree coefficients $a_{m,n}, b_{m,n}$ for n closed to $\widetilde{N}$.

The above question has a positive answer in the the case when (i) one has to compute the values of a spherical polynomial Y_N with "small" high degree coefficients and (ii) the error must not exceed ε which is within some reasonable bound depending on the smoothness of Y_N (not arbitrarily small). Being able to reduce significantly the size of M allows to utilize our method for fast compressed (memory efficient) evaluation of spherical polynomials with tight control on the accuracy. This is precisely the case described in Example 2 in §5.

4.3. **Application to other problems.** The operators Φ_N from (2.29) and their truncated versions $\Phi_{N,\delta}$ in (2.30) are a powerful *approximation tool* as evidenced by estimates (2.36) in Theorem 2.3 and (2.43) in Theorem 2.4. Note that condition (2.34) is no longer needed when these operators are used for approximation. Rather, the identity $N = \lfloor M/(2+\tau)\rfloor$ can be used to define the parameter N appearing in the right-hand sides of (2.36) and (2.43).

The superb localization of the kernels of the operators Φ_N and $\Phi_{N,\delta}$ and their compatibility with spherical harmonics make them an excellent tool for global as well as local approximation. The latter is a desirable feature for practical applications. Here "local" means that the approximant is closer to the approximated function in regions where the function is smoother than globally. This is a well known fact in the classical approximation theory.

Formulas (2.29) and, especially, (2.30) can be viewed as "interpolation" formulas, and hence used for *fast generation of surfaces in computer-aided geometric design.*

Our algorithm can also be used for *fast verification* whether given data represent (within accuracy ε_0) the values at given regular grid points of some (unknown) spherical polynomial of degree N. The criterion is defined by

$$|f(\xi) - \Phi_{N,\delta} f(\xi)| \le \varepsilon_0 \quad \forall \xi \in \mathcal{X},$$

where $f(\xi)$ denotes the value at ξ and δ is calculated for ε defined in (3.1). In this case the grid should be oversampled with respect to the polynomial degree.

Applications of the spherical "father needlets" to reconstruction of band-limited functions from their values at scattered points on the sphere are given in Ivanov, Petrushev [11].

5. Numerical experiments

The method for evaluation of high degree spherical polynomials at scattered points described in this article has been implemented in software written initially in MATLAB 7.2 and then rewritten in MATLAB 2012b with double-precision variables. Variable precision arithmetic has not been used in the code.

Our experiments were conducted in real time on a small 1.6 GHz PC with 1 GB of RAM and on a 3.4 GHz PC with 16 GB of RAM. The method has been intensively tested for degrees between 500 and 2190. The verification of experiments with high degree spherical polynomials is not easy for lack of independent reliable software.

For instance, the MATLAB function `legendre(n,X,'norm')` gives wrong answers (including 0 or NaN) for degrees $n > 3000$.

We have also made a number of experiments with spherical polynomials of degrees up to 10 000 and compared the results with the results of code performing sharp direct computations in variable precision arithmetic. Unfortunately, such code is too slow for any substantial testing. In all experiments the results were in full agreement with the theory.

Here we report the result of two experiments with our method: the first with spherical polynomials of "large" high degree coefficients, and the second with the spherical polynomial representing the geoid undulation in the 2160 model of NGA (EGM2160) with relatively small high degree coefficients.

Example 1. For $n = 500$, $n = 1\ 000$ and $n = 2\ 000$ let F_n be defined by

$$F_n(\theta,\lambda) := 0.5q_{0,n}P_{0,n}(\cos\theta) + \sum_{m=1}^{n} q_{m,n}P_{m,n}(\cos\theta)\cos(m\lambda)$$

with $q_{m,n}$ given by (2.7). F_n has relatively small values in the interiors of the domains $\{(\theta,\lambda) : 0 < \theta < \frac{\pi}{2}, \frac{\pi}{2} < \lambda < \frac{3\pi}{2}\}$ and $\{(\theta,\lambda) : \frac{\pi}{2} < \theta < \pi, -\frac{\pi}{2} < \lambda < \frac{\pi}{2}\}$. The extrema of F_n are localized around $(\frac{\pi}{2}, \frac{\pi}{2})$ and $(\frac{\pi}{2}, \frac{3\pi}{2})$. The values of F_{500} on an 1601×3200 grid range from -451.959 to 479.493. The graph of F_{500} in spherical coordinates is given in Figure 3.

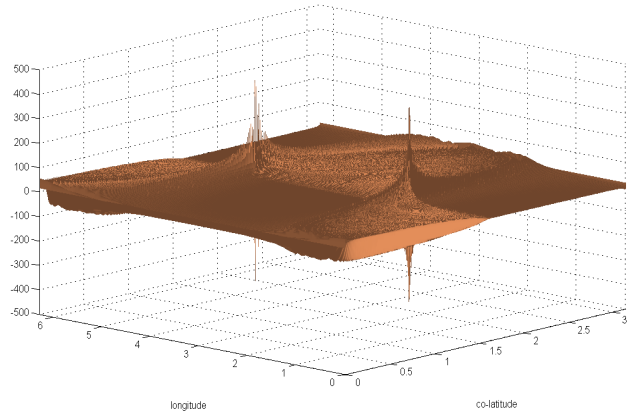

FIGURE 3. Graph of F_{500}

A representative of the behavior of F_n is the region $\mathcal{D} = \{(\theta,\lambda) : |\frac{\pi}{2} - \theta| \le \frac{\pi}{15}, |\pi - \lambda| \le \frac{2\pi}{15}\}$, where we have high oscillation in the longitude direction and essential decrease of the absolute value in the latitude direction. The values of F_{500} in $\mathcal{D}$ range from -22.616 to 22.892. The graph of F_{500} over this rectangle is given in Figure 4.

Our experiments have shown full agreement of the test results with the theory. The error of computation was within the prescribed bound ε_0 for $\varepsilon_0 = 10^{-5}$, 10^{-6}, 10^{-7}, 10^{-8}, 10^{-9}, 10^{-10} in all cases, whereas ε in (3.1) was determined by $\|F_{500}\|_{\ell^\infty} = 480$ for $(\theta,\lambda) \in [0,\pi] \times [0,2\pi)$ and by $\|F_{500}\|_{\ell^\infty} = 23$ for $(\theta,\lambda) \in \mathcal{D}$.

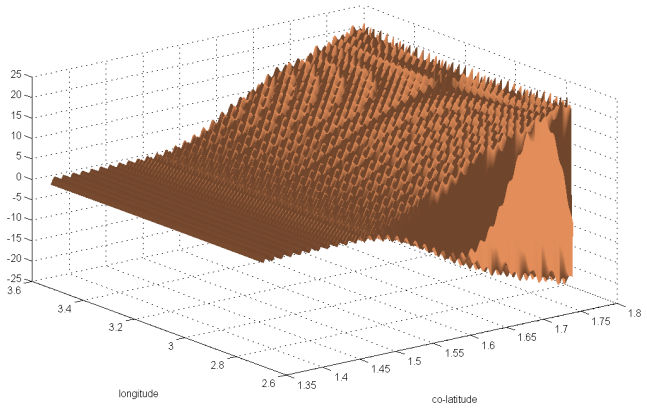

FIGURE 4. Graph of F_{500} over $\mathcal{D}$

The later increase of ε is allowed by the local nature of the operators. The errors in evaluating F_n for $n = 1\ 000$ and $n = 2\ 000$ are almost the same as for F_{500}.

Experiments with parameters satisfying conditions (A) and/or (B) of §4.2 showed that for $\varepsilon_0 = 10^{-10}$ practically no significant reduction of speed is possible. On the other hand a gain of speed by a factor of two is possible for $\varepsilon_0 = 10^{-5}$ (depending on the number of grid points). Under similar ratios in conditions (A) and (B) the contribution of condition (A) to the error was higher than the contribution of condition (B).

Example 2. The geoid undulation $\mathcal{G}$ is approximated by a spherical polynomial of degree and order $\widetilde{N} = 2189$, computed in the official Earth Gravitational Model EGM2008 and publicly released by the U.S. National Geospatial-Intelligence Agency (NGA). The polynomial coefficients have been taken from

`http://earth-info.nga.mil/GandG/wgs84/gravitymod/egm2008/egm08_wgs84.html`.

This website also contains the values of the geoid undulation on two mesh grids of type (2.1): $2.5' \times 2.5'$ (i.e. $K = M = 4320$, $L = 8640$) and $1' \times 1'$ (i.e. $K = M = 10800$, $L = 21600$). The $1' \times 1'$ grid points are $233,301,600$. The geoid undulation values as single precision numbers occupy 890MB on the hard disk and range from -106.9 m to 85.8 m.

Table 4 summarizes the results of the testing. The following programs are compared:

- `hsynth_WGS84` – the NGA spherical harmonic synthesis program computing $\mathcal{G}$ by its coefficients directly from (2.12); written in FORTRAN; for comparison purposes assumed to be exact, so the error reported in Table 4 is 0.
- `interp_1min` – the NGA spherical harmonic synthesis program computing $\mathcal{G}$ by spline interpolation of the $1' \times 1'$ undulation data; written in FORTRAN; because of the higher memory requirements, the code was tested only on a 16 GB RAM computer.

- `interp_2p5min` – the NGA spherical harmonic synthesis program computing $\mathcal{G}$ by spline interpolation of the $2.5' \times 2.5'$ undulation data; written in FORTRAN.
- `needlet3` – implementation of our algorithm which uses the $3' \times 3'$ undulation data; written in MATLAB.
- `needlet4` – implementation of our algorithm which uses the $4' \times 4'$ undulation data; written in MATLAB.

Program	Size HD (MB)	Size RAM (MB)	values/ second	Error (mm)
`hsynth_WGS84`	71.2	53.9	16	0
`interp_1min`	890.0	1 814.0	640 000	0.84
`interp_2p5min`	142.5	287.6	630 000	3.52
`needlet3`	70.9	132.4	11 000	0.40
`needlet4`	41.1	100.2	4 400	0.36

TABLE 4. Program comparison by memory size, speed (on a 3.4 GHz PC) and error

In Table 4 the column "Size HD" indicates the space on HD needed for storing the grid values, while "Size RAM" shows the amount of RAM needed for both the grid values and work variables. The NGA programs `interp_1min` and `interp_2p5min` require approximately 20 and 7 seconds for loading into the memory and initialization, while each of `needlet3` or `needlet4` requires approximately 2 seconds. The total run time should be formed as the sum of these values, the time for reading scattered point coordinates and writing polynomial values on HD plus the time for proper point evaluation, which can be computed using column "values/second". The column "Error" indicates the maximal point-wise deviation of the computed values compared to the values computed by `hsynth_WGS84`.

Program `hsynth_WGS84` solves Problem 1 while the remaining programs solve Problem 3 described in §2.1.

The sampling interval for the Nyquist frequency is $\pi/2160 = 5'$ and programs `needlet3` and `needlet4` work with $3' \times 3'$ and $4' \times 4'$ mesh grids producing results with relative error approximately $\varepsilon = 4 \cdot 10^{-6}$. These programs demonstrate that for some quantities used in practice one can violate (2.34) as discussed in §4.2 and still achieve very good approximation. The point is that the geoid undulation has smoothness which makes possible on the one hand the data compression by `needlet3` and `needlet4` and on the other the better approximation by `interp_1min` compared to `interp_2p5min`. The needlet software in this example is optimized to give best speed using polynomial values at relatively sparse predefined grids, while keeping the computational error under the limit of 0.5 mm.

As explained before one can increase the accuracy of the needlet software by simply increasing δ and using the same grid values. Thus polynomial evaluation at additional grid points is not needed. This is not the case when using spline interpolation; the program `interp_1min` uses many more points than `interp_2p5min`.

The test results described in Table 4 show that `needlet3` and `needlet4` are memory efficient and, therefore, they can be effectively used for fast compressed and accurate computation of the geoid undulation at scattered points on the sphere.

This is the main advantage of `needlet3` and `needlet4` over `interp_1min`. Of course, as usual here there is a trade-off between memory size and speed.

Observe also that we use the same algorithm for both Example 1 and Example 2. In contrast, the spline interpolation software discussed above looses accuracy when evaluating functions as in Example 1 because of their rapid oscillation.

The values reported in Table 4 for the speed and accuracy of `interp_1min` and `interp_2p5min` are computed when bi-variate interpolating sixth order splines are used for approximation. Further increase of the spline order does not give better accuracy in the case of $2.5'$ spline interpolation, while the accuracy improves in the case of $1'$ spline interpolation. The optimal observed order when using `interp_1min` is 10 and the accuracy improves to 0.1 mm; the speed drops twice.

To compare the performance of different programs on different examples it is convenient to measure the accuracy in terms of relative error with respect to the polynomial norm, cf. (3.1). Thus the accuracy 0.1 mm reported above represents relative error of 10^{-6}. The problem with spline interpolation is that it is not sufficiently accurate when applied to spherical polynomials with large high degree (frequency) coefficients. For example, the relative error of the result when `interp_1min` is applied to the polynomial from Example 1 with $n = 2160$ is larger than 0.2×10^{-3} for all orders (up to 20) of the interpolating splines, which is not quite satisfactory. Geodetic quantities represented by spherical polynomials with large high degree coefficients in the NGA model are for instance the gravity anomaly second radial derivative and the spherically approximated north-south and east-west vertical deflections. The needlet algorithm does not have this drawback.

6. Discussion

In the paper we have presented a method for fast and memory efficient evaluation within any precision of high degree spherical polynomials at many scattered points on the sphere. As shown in §4.3 the method can also be used for approximation on the sphere, for verification of spherical polynomials, and for fast generation of surfaces in computer-aided geometric design.

The strength of the operator $\Phi_{N,\delta}$ can be summarized as follows:

- *Excellent approximation* properties
  - The spherical polynomials $\{w_\xi \mathcal{K}_N(\xi \cdot x) : \xi \in \mathcal{X}\}$ form not only a *superbly localized partition of unity* but also reproduce the N-th degree spherical polynomials. As a consequence we have inequality (2.43).
- *Numerical stability*
  - The operator norm $\|\Phi_{N,\delta}\|_{\ell^\infty(\mathcal{X})\to L^\infty(\mathbb{S}^2)}$ is between 2.5 and 4.5 for the values of τ and ε under consideration (see [11]). Thus, the error generated in evaluating function values $f(\xi), \xi \in \mathcal{X}$, is kept bounded, which is *stability by initial data.*
  - The rounding errors in computing $\Phi_{N,\delta} f(x)$ have small impact on the outcome because the rapid decay of $\mathcal{K}_N(\xi \cdot x)$ implies that the summands in (2.30) are of different magnitudes. Hence, the prescribed accuracy in uniform norm, which is guaranteed by theory, is achieved in practice too.
- *Fast evaluation*
  - Only functional values at the nodes from a *δ-neighborhood* of a point x are used in the computation of $\Phi_{N,\delta} f(x)$.

  - The kernel $\mathcal{K}_N(\xi \cdot x)$ is a superposition of a dot product and a univariate function, i.e. a *ridge function*, which allows fast computation.
- Mild requirements on the nodal sets
  - The nodal set should allow: (i) the construction of a cubature with positive weights that is exact for M-th degree spherical polynomials; (ii) fast determination of the nodes from a δ-neighborhood of any point.
  - This allows a wide variety of nodal sets to be used.
  - The algorithm can work with, but *does nor require*, asymptotically equally spaced nodes, such as the ones given by HEALPix or GLESP. In these cases, however, the construction of cubatures which are exact for high degree spherical polynomials is problematic.

Some other distinctive features of our algorithm are:

- The product $N\delta$ depends logarithmically on ε_0, which allows the algorithm to work with *practically the same speed* for widely varying precisions ε_0. At the same time the speed *does not depend on the polynomial degree*. Thus very high degrees and very fine precisions are attainable for effective computation.
- The algorithm error is measured in the *uniform norm*, which guarantees the computational accuracy at any point from the sphere. This feature gives our algorithm an important advantage over algorithms with error estimates in average, in RMS or of statistical nature.
- The *local* nature of formula (2.30) implies that only nodes which are close to the point of interest enter the computations, even if the polynomial is highly oscillating (see Example 1 in §5). As a consequence, when computations for a given region are performed only the grid points covering the region plus a small neighborhood have to be stored in the computer memory.
- The local nature of the method also leads to its *natural parallelization*.
- The improvement of the precision ε_0 is achieved by increasing δ and *does not require* computation of polynomial values at new nodal points. Such increase of δ does not affect the computed approximation for the previous δ, thus an application of the algorithm in a nested fashion may be used for gaining speed (see §3.6).
- One of the main ways for increasing the speed of the algorithm is by increasing the parameter τ as (3.19) and (3.38) show. Under certain conditions τ can be chosen larger than the main restriction from (2.34) allows (see §4.2 and Example 2 of §5).
- For a given nodal set $\mathcal{X}$ one can use different cubatures satisfying the common requirement of high degree of exactness.
- The method successfully *avoids underflow and overflow* problems since no evaluation of a single associated Legendre function is performed. We only use downward Clenshaw summation with the Legendre polynomials recurrence.
- The advantage of our algorithm for solving Problem 3 from §2.1 over the direct computation of (2.12) for solving Problem 1 (implemented, for example, in `hsynth_WGS84`) becomes significant for spherical polynomials of degree 300 or higher.

7. Appendix: Localization of reproducing Jacobi polynomial kernels

We first construct cutoff functions with small derivatives. Denote by $\mathcal{N}_k$ the normalized B-spline with knots $0, 1, \dots, k$, defined by convolving k times the characteristic function $\chi_{[0,1]}$ of the interval $[0,1]$, i.e.

$$\mathcal{N}_k = \underbrace{\chi_{[0,1]} * \cdots * \chi_{[0,1]}}_{k-\text{times}}. \tag{7.1}$$

From (7.1) we get $\mathcal{N}_k(t) > 0$ for $t \in (0,k)$, $\mathcal{N}_k(t) = 0$ for $t \in \mathbb{R}\backslash(0,k)$ and

$$\int_0^k \mathcal{N}_k(v)\,dv = 1. \tag{7.2}$$

In order to estimate the uniform norm of $\mathcal{N}_k$ and its derivatives we first derive from (7.1) and the Fourier transform of $\chi_{[0,1]}$

$$\|\mathcal{N}_k\|_{L^\infty(\mathbb{R})} = \mathcal{N}_k(k/2) = \pi^{-1}\int_{-\infty}^{\infty}\left(\frac{\sin\pi\omega}{\pi\omega}\right)^k d\omega = \sqrt{\frac{6}{\pi^3 k}}(1+o(1)).$$

Also (7.1) gives $\mathcal{N}_k'(x) = \mathcal{N}_{k-1}(x) - \mathcal{N}_{k-1}(x-1)$, which implies

$$\begin{aligned}\|\mathcal{N}_k^{(k-1)}\|_{L^\infty(\mathbb{R})} &= \Big\|\sum_{j=0}^{k-1}(-1)^j\binom{k-1}{j}\chi_{[j,j+1]}\Big\|_{L^\infty(\mathbb{R})}\\ &= \max_{0\le j\le k-1}\binom{k-1}{j} = 2^{k-1}\sqrt{\frac{2}{\pi k}}(1+o(1)).\end{aligned}$$

Now the Kolmogorov-Landau inequality (see Theorem 7.1 in Chapter 5 of [2, p. 153]) yields

$$\|\mathcal{N}_k^{(\ell-1)}\|_{L^\infty(\mathbb{R})} \le \mu_k 2^\ell, \quad \ell = 1,2,\dots,k, \tag{7.3}$$

where $\mu_k = c^* k^{-1/2}$ with c^* an absolute constant.

We use the normalized B-spline $\mathcal{N}_k$ from above to define the cutoff function

$$\varphi(t) = \int_{t-1-\tau/2}^{\tau/2} 2k\tau^{-1}\mathcal{N}_k(2k\tau^{-1}s)\,ds, \quad t\in[0,\infty). \tag{7.4}$$

Clearly, $\varphi(t) = 1$ for $t \in [0, 1+\tau/2]$, $\varphi(t) = 0$ for $t \in [1+\tau, \infty)$, i.e. φ is a cutoff function. Furthermore, (7.1) implies that $\varphi \in C^{k-1}[0,\infty)$ and $\varphi^{(k-1)}$ is a piece-wise linear continuous function. Hence $\varphi \in W^k_\infty[0,\infty)$.

The Jacobi polynomials $\{P_n^{(\alpha,\beta)}\}_{n\ge 0}$ form an orthogonal basis for the weighted space $L^2([-1,1], w_{\alpha,\beta})$ with weight $w_{\alpha,\beta}(x) := (1-x)^\alpha(1+x)^\beta$, $\alpha,\beta > -1$, and are traditionally normalized by $P_n^{(\alpha,\beta)}(1) = \binom{n+\alpha}{n}$. It is well known that [26, (4.3.3)]

$$\int_{-1}^{1} P_n^{(\alpha,\beta)}(x)P_m^{(\alpha,\beta)}(x)w_{\alpha,\beta}(x)dx = \delta_{n,m}h_n^{(\alpha,\beta)},$$

where

$$h_n^{(\alpha,\beta)} = \frac{2^{\alpha+\beta+1}}{(2n+\alpha+\beta+1)}\frac{\Gamma(n+\alpha+1)\Gamma(n+\beta+1)}{\Gamma(n+1)\Gamma(n+\alpha+\beta+1)}. \tag{7.5}$$

We are interested in kernels of the form

$$\mathcal{Q}_N^{\alpha,\beta}(x,y) = \sum_{n=0}^{\infty} \varphi\Big(\frac{n}{N}\Big)\Big(h_n^{(\alpha,\beta)}\Big)^{-1} P_n^{(\alpha,\beta)}(x)P_n^{(\alpha,\beta)}(y), \quad x,y\in[-1,1], \tag{7.6}$$

where φ is a cutoff function, i.e. $\varphi(t)=1$ for $t\in[0,1]$ and $\varphi(t)=0$ for $t\in[1+\tau,\infty)$. Set

$$\mathcal{K}_N^{\alpha,\beta}(x) := \mathcal{Q}_N^{\alpha,\beta}(x,1) = \sum_{n=0}^{\infty} \varphi\Big(\frac{n}{N}\Big)\Big(h_n^{(\alpha,\beta)}\Big)^{-1} P_n^{(\alpha,\beta)}(x)P_n^{(\alpha,\beta)}(1). \tag{7.7}$$

It is easy to see that

$$\mathcal{K}_N^{\alpha,\beta}(x) = c^\star \sum_{n=0}^{\infty} \varphi\Big(\frac{n}{N}\Big)\frac{(2n+\alpha+\beta+1)\Gamma(n+\alpha+\beta+1)}{\Gamma(n+\beta+1)}P_n^{(\alpha,\beta)}(x), \tag{7.8}$$

where $c^\star := 2^{-\alpha-\beta-1}\Gamma(\alpha+1)^{-1}$. Here the product $(2n+\alpha+\beta+1)\Gamma(n+\alpha+\beta+1)$ for $n=0$ is replaced by $\Gamma(\alpha+\beta+2)$.

A localization estimate of the kernel $\mathcal{K}_N^{\alpha,\beta}$ for φ defined in (7.4) is given in

Theorem 7.1. *Let $N,k\in\mathbb{N}$, $N>k$ and $\tau>0$. Then for any $\alpha\ge\beta\ge -1/2$ there exist constants $c_0,c_1>0$ depending only on α,β such that*

$$|\mathcal{K}_N^{\alpha,\beta}(\cos\theta)| \le c_0\,((1+\tau)N)^{2\alpha+2}\min\left\{1,\left(\frac{c_1 k}{\tau N\theta}\right)^k\right\}, \quad \theta\in[0,\pi]. \tag{7.9}$$

Proof. We shall need the simple inequality

$$\Gamma(n+\alpha+k+\beta+1)/\Gamma(n+\beta+1) \le c(n+k)^{\alpha+k}, \quad c=c(\alpha,\beta). \tag{7.10}$$

A trivial estimate of $|\mathcal{K}_N^{\alpha,\beta}|$ follows by applying $\|P_n^{(\alpha,\beta)}\|_{L^\infty[-1,1]} \le cn^\alpha$ with $c=c(\alpha,\beta)$ [26, (7.32.6)] and (7.10) with $k=0$ in (7.8)

$$|\mathcal{K}_N^{\alpha,\beta}(\cos\theta)| \le c\left(1+\sum_{1\le n<(1+\tau)N} n^{2\alpha+1}\right) \le c((1+\tau)N)^{2\alpha+2}, \quad c=c(\alpha,\beta). \tag{7.11}$$

A key role in obtaining a nontrivial estimate on $|\mathcal{K}_N^{\alpha,\beta}|$ will play the identity [26, (4.5.3)]:

$$\begin{aligned}\sum_{\nu=0}^{n} \frac{(2\nu+\alpha+m+\beta+1)\Gamma(\nu+\alpha+m+\beta+1)}{\Gamma(\nu+\beta+1)}P_\nu^{(\alpha+m,\beta)}(x)\\ = \frac{\Gamma(n+\alpha+m+1+\beta+1)}{\Gamma(n+\beta+1)}P_n^{(\alpha+m+1,\beta)}(x).\end{aligned} \tag{7.12}$$

Applying summation by parts to the sum in (7.8) using (7.12) with $m=0$, we get

$$\mathcal{K}_N^{\alpha,\beta}(x) = c^\star \sum_{n=0}^{\infty}\Big[\phi\Big(\frac{n}{N}\Big)-\phi\Big(\frac{n+1}{N}\Big)\Big]\frac{\Gamma(n+\alpha+1+\beta+1)}{\Gamma(n+\beta+1)}P_n^{(\alpha+1,\beta)}(x). \tag{7.13}$$

In order to apply repeatedly summation by parts to the sum in (7.13) we define the sequence of functions $\{A_m(u)\}_{m=0}^{\infty}$, $u\in[0,\infty)$, recursively by

$$A_0(u):=\phi\left(\frac{u}{N}\right),\quad A_m(u):=\frac{A_{m-1}(u)-A_{m-1}(u+1)}{2u+\alpha+m+\beta+1},\quad m\geq 1. \tag{7.14}$$

Note that (7.14) for $m=1$ is

$$A_1(u):=\frac{\phi\left(\frac{u}{N}\right)-\phi\left(\frac{u+1}{N}\right)}{2u+\alpha+1+\beta+1}, \tag{7.15}$$

which implies $\operatorname{supp} A_1\subset[(1+\tau/2)N-1,(1+\tau)N]$. Inductively we get $\operatorname{supp} A_m\subset[(1+\tau/2)N-m,(1+\tau)N]$. With this notation we rewrite (7.13) as

$$\mathcal{K}_N^{\alpha,\beta}(x)=c^\star\sum_{n=0}^{\infty}A_1(n)\frac{(2n+\alpha+1+\beta+1)\Gamma(n+\alpha+1+\beta+1)}{\Gamma(n+\beta+1)}P_n^{(\alpha+1,\beta)}(x). \tag{7.16}$$

Applying summation by parts $k-1$ times starting from (7.16) (using every time (7.12)), we arrive at the identity:

$$\mathcal{K}_N^{\alpha,\beta}(x)=c^\star\sum_{n=0}^{\infty}A_k(n)\frac{(2n+\alpha+k+\beta+1)\Gamma(n+\alpha+k+\beta+1)}{\Gamma(n+\beta+1)}P_n^{(\alpha+k,\beta)}(x). \tag{7.17}$$

The summation index n in (7.17) effectively runs from $\lfloor(1+\tau/2)N\rfloor-k+1$ to $\lceil(1+\tau)N\rceil-1$ because $A_k(n)=0$ for the other n's.

We next prove the estimates

$$\|A_m^{(\ell)}\|_{L^\infty[0,\infty)}\leq\mu_k\frac{2^{3m+2\ell}k^{m+\ell}}{\tau^{m+\ell}(1+\tau)^mN^{2m+\ell}} \tag{7.18}$$

for all $\ell,m\geq 0$ in the range $0<m+\ell\leq k$, where μ_k is from (7.3).

Let $m=0$. For $\ell=1$ we have

$$A_0'(u)=N^{-1}\varphi'(uN^{-1})=-2k(\tau N)^{-1}\mathcal{N}_k(2k\tau^{-1}(uN^{-1}-1-\tau/2)).$$

Hence $A_0^{(\ell)}(u)=-(2k/(\tau N))^\ell\mathcal{N}_k^{(\ell-1)}(2k\tau^{-1}(uN^{-1}-1-\tau/2))$ and using (7.3) we get

$$\|A_0^{(\ell)}\|_{L^\infty[0,\infty)}\leq\mu_k\left(\frac{4k}{\tau N}\right)^\ell,\quad \ell=1,2,\dots,k,$$

which is (7.18) for $m=0$.

We prove (7.18) for $m\geq 1$ by induction on m and for every m by induction on ℓ. We rewrite (7.14) as

$$(2u+\alpha+m+\beta+1)A_m(u)=-\int_0^1 A_{m-1}'(u+v)\,dv. \tag{7.19}$$

The ℓ-th derivative of the above representation by Leibniz identity gives

$$A_m^{(\ell)}(u)=-\frac{2\ell A_m^{(\ell-1)}(u)+\int_0^1 A_{m-1}^{(\ell+1)}(u+v)\,dv}{2u+\alpha+m+\beta+1}. \tag{7.20}$$

As indicated above $A_m(u)=0$ for $u\leq(1+\tau/2)N-m$. Therefore, in the proof of (7.18) we use (7.20) for $u>(1+\tau/2)N-m$. Since $N>k\geq m$ for these u's we have $2u+\alpha+m+\beta+1\geq(1+\tau)N$.

Assume that (7.18) is established for $m-1$. Then (7.19) gives

$$\|A_m\|_{L^\infty[0,\infty)} \le \frac{1}{(1+\tau)N}\mu_k \frac{2^{3(m-1)+2}k^{m-1+1}}{\tau^m(1+\tau)^{m-1}N^{2(m-1)+1}} = \frac{1}{2}\mu_k\frac{2^{3m}k^m}{\tau^m(1+\tau)^m N^{2m}},$$

which implies (7.18) for $\ell=0$. For $\ell=1,2,\dots,k-m$ we get from (7.20)

$$\begin{aligned}&\|A_m^{(\ell)}\|_{L^\infty[0,\infty)}\\ &\quad\le \frac{1}{(1+\tau)N}\mu_k\left(2\ell\frac{2^{3m+2\ell-2}k^{m+\ell-1}}{\tau^{m+\ell-1}(1+\tau)^m N^{2m+\ell-1}} + \frac{2^{3m+2\ell-1}k^{m+\ell}}{\tau^{m+\ell}(1+\tau)^{m-1}N^{2m+\ell-1}}\right)\\ &\qquad= \mu_k\left(\frac{\ell\tau}{2k(1+\tau)}+\frac{1}{2}\right)\frac{2^{3m+2\ell}k^{m+\ell}}{\tau^{m+\ell}(1+\tau)^m N^{2m+\ell}} < \mu_k\frac{2^{3m+2\ell}k^{m+\ell}}{\tau^{m+\ell}(1+\tau)^m N^{2m+\ell}},\end{aligned}$$

where the last inequality follows from $\ell\le k-1$. This proves (7.18).

We shall need the following estimate for Jacobi polynomials [5, Theorem 1]: For $\alpha,\beta\ge -1/2$ and $n\ge 1$,

$$\sup_{x\in[-1,1]}(1-x)^{\alpha+1/2}(1+x)^{\beta+1/2}|P_n^{(\alpha,\beta)}(x)|^2 \le \frac{2e}{\pi}\big(2+\sqrt{\alpha^2+\beta^2}\big)h_n^{(\alpha,\beta)}, \tag{7.21}$$

where $h_n^{(\alpha,\beta)}$ is from (7.5).

By (7.5) it readily follows that

$$h_n^{(\alpha+k,\beta)} \le c2^k n^{-1}. \tag{7.22}$$

Using (7.22), (7.21), and the obvious inequalities $1-\cos\theta\ge 2\pi^{-2}\theta^2$, $1+\cos\theta\ge 1$ for $0<\theta\le\pi/2$, we infer

$$|P_n^{(\alpha+k,\beta)}(\cos\theta)| \le \frac{ck^{1/2}\pi^k}{n^{1/2}\theta^{k+\alpha+1/2}}, \quad 0<\theta\le\pi/2. \tag{7.23}$$

We now use (7.18) with $m=k$ and $\ell=0$, (7.10) and (7.23) in (7.17) to obtain for $0<\theta\le\pi/2$ and $N>k$

$$\begin{aligned}&|\mathcal{K}_N^{\alpha,\beta}(\cos\theta)| \qquad (7.24)\\ &\quad\le c\sum_{(1+\tau/2)N-k\le n<(1+\tau)N}\mu_k\frac{2^{3k}k^k}{\tau^k(1+\tau)^k N^{2k}}n(n+k)^{\alpha+k}\frac{k^{1/2}\pi^k}{n^{1/2}\theta^{k+\alpha+1/2}}\\ &\qquad\le c_0((1+\tau)N)^{2\alpha+2}\left(\frac{c_1k}{\tau N\theta}\right)^{k+\alpha+1/2} \le c_0((1+\tau)N)^{2\alpha+2}\left(\frac{c_1k}{\tau N\theta}\right)^k\end{aligned}$$

whenever $c_1k\le\tau N\theta$. Now, (7.11) and (7.24) yield (7.9) for $0\le\theta\le\pi/2$.

Now let $\pi/2\le\theta\le\pi-1/N$. Using (7.22), (7.21), and the obvious inequalities $1+\cos\theta\ge 2\pi^{-2}(\pi-\theta)^2\ge 2(\pi N)^{-2}$, $1-\cos\theta\ge 1$ for these θ's we infer

$$|P_n^{(\alpha+k,\beta)}(\cos\theta)| \le \frac{ck^{1/2}2^{k/2}}{n^{1/2}(\pi-\theta)^{\beta+1/2}} \le c2^k n^{-1/2}N^{\beta+1/2}, \quad \frac{\pi}{2}\le\theta\le\pi-\frac{1}{N}. \tag{7.25}$$

Using (7.25) instead of (7.23) in the proof of (7.24) we get

$$|\mathcal{K}_N^{\alpha,\beta}(\cos\theta)| \le \tilde{c}_0(1+\tau)^{\alpha+3/2}N^{\alpha+\beta+2}\left(\frac{\tilde{c}_1k}{\tau N}\right)^k,$$

which implies

$$\|\mathcal{K}_N^{\alpha,\beta}\|_{C[\cos(\pi-1/N),0]} \le \tilde{c}_0((1+\tau)N)^{2\alpha+2}\left(\frac{\tilde{c}_1 k}{\tau N}\right)^k.$$

This estimate combined with (3.5) and $\mathcal{K}_N^{\alpha,\beta} \in \Pi_{(1+\tau)N}$ implies

$$\|\mathcal{K}_N^{\alpha,\beta}\|_{C[-1,0]} \le c_0((1+\tau)N)^{2\alpha+2}\left(\frac{\tilde{c}_1 k}{\tau N}\right)^k,$$

which completes the proof of the theorem. □

Acknowledgements. The authors would like to thank the referees for their valuable remarks and comments.

References

[1] C. W. Clenshaw, A. R. Curtis, A method for numerical integration on an automatic computer, Numer. Math., **2** (1960), 197–205.
[2] R. DeVore,J. Lorentz, *Constructive Approximation*, Springer, Berlin, 1993.
[3] J. R. Driscoll, D. M. Healy, Computing Fourier Transforms and Convolutions on the 2-Sphere, Adv. in Appl. Math., **15** (1994), 202–250.
[4] A. Dutt and V. Rokhlin. Fast Fourier transforms for nonequispaced data. SIAM J. Sci. Stat. Comput., **14** (1993), 1368–1393.
[5] T. Erdelyi, A. Magnus and P. Nevai, Generalized Jacobi weights, Christoffel functions, and Jacobi polynomials, SIAM J. Math. Anal., **25** (1994), 602–614.
[6] A. Erdélyi, W. Magnus, F. Oberhettinger and F. G. Tricomi, *Higher Transcendental Functions*, Vol. **2**, McGraw-Hill, New York, 1953.
[7] L. Fejér, On the infinite sequences arising in the theories of harmonic analysis, of interpolation, and of mechanical quadratures, Bull. Amer. Math. Soc., **39** (1933), 521–534.
[8] L. Fejér, Mechanische Quadraturen mit positiven Cotesschen Zahlen, Math. Z., **37** (1933), 287–309.
[9] Z. Gimbutas, L. Greengard, A fast and stable method for rotating spherical harmonic expansions, J. Comput. Phys., **228** (2009), 5621–5627.
[10] A. Glaser, X. Liu, V. Rokhlin, A fast algorithm for the calculation of the roots of special functions, SIAM Journal on Scientific Computing, **29** (2007), 1420–1438.
[11] K. G. Ivanov, P. Petrushev, Irregular sampling of band-limited functions on the sphere and in more general settings, 2013, preprint. http://imi.cas.sc.edu/papers/
[12] K. G. Ivanov, P. Petrushev, Y. Xu, Sub-exponentially localized kernels and frames induced by orthogonal expansions, Math. Z., **264** (2010), 361–397.
[13] K. G. Ivanov, P. Petrushev, Y. Xu, Decomposition of spaces of distributions induced by tensor product bases, J. Funct. Anal., **263** (2012), 1147–1197.
[14] K. G. Ivanov, V. Totik, Fast decreasing polynomials, Constructive Approximation, **6** (1989), 1–21.
[15] S. Kunis, D. Potts, Fast spherical Fourier algorithms, J. Comput. Appl. Math., **161** (2003), 75–98.
[16] M.-J. Lai, L. Schumaker, *Spline Functions on Triangulations*, Cambridge University Press, 2007.
[17] M. Mohlenkamp, A Fast Transform for Spherical Harmonics, J. Fourier Anal. Appl., **5** (1999), 159–184.
[18] H. Moritz, B. Hofmann-Wellenhof, *Physical Geodesy*, Springer Wein New York Publishing, 2006.
[19] F. J. Narcowich, P. Petrushev and J. D. Ward, Localized tight frames on spheres, SIAM J. Math. Anal., **38** (2006), 574–594.
[20] F. J. Narcowich, P. Petrushev and J. D. Ward, Decomposition of Besov and Triebel-Lizorkin spaces on the sphere, J. Funct. Anal., **238** (2006), 530-564.
[21] P. Nevai, *Orthogonal Polynomials*, Memoirs of AMS, Vol. **18**, 1979.

[22] N. K. Pavlis, S. A. Holmes, S .C. Kenyon, and J. K. Factor, An Earth Gravitational Model to Degree 2160: EGM2008, presented at the 2008 General Assembly of the European Geosciences Union, Vienna, Austria, April 13-18, 2008.

[23] M. G. Reuter, M. A. Ratner, and T. Seideman, A fast method for solving both the time-dependent Schroedinger equation in angular coordinates and its associated 'm-mixing' problem, The Journal of Chemical Physics, **131** (094108), 1-6, 2009. doi:10.1063/1.3213436.

[24] D. S. Seljebotn, Wavemoth – fast spherical harmonic transforms by butterfly matrix compression, The Astrophysical Journal Supplement Series, **199** (1-5), 1-12, 2012. doi:10.1088/0067-0049/199/1/5.

[25] E. Stein, G. Weiss, *Fourier analysis on Euclidean spaces*, Princeton University Press, Princeton, New Jessey, 1971.

[26] G. Szegő, *Orthogonal Polynomials*, Amer. Math. Soc. Colloq. Publ. Vol. **23**, Providence, 4th edition, 1975.

[27] L. N. Trefethen, and others. Chebfun Version 4.2, The Chebfun Development Team, (2011) http://www.maths.ox.ac.uk/chebfun/.

[28] M. Tygert, Fast algorithms for spherical harmonic expansions, II, J. Comput. Phys., **227** (2008), 4260–4279.

[29] M. Tygert, Fast algorithms for spherical harmonic expansions, III, J. Comput. Phys., **229** (2010), 6181–6192.

Institute of Mathematics and Informatics, Bulgarian Academy of Sciences, 1113 Sofia, Bulgaria

E-mail address: kamen@math.bas.bg

Department of Mathematics, University of South Carolina, Columbia, SC 29208, and Institute of Mathematics and Informatics, Bulgarian Academy of Sciences

E-mail address: pencho@math.sc.edu